

Recent advances of Imide-functionalized polymer Donors for Non-fullerene Solar Cells

Huijuan Wang¹, Songmin Mo¹, Dongyan Li¹, and Qinghe Wu¹

¹Shantou University

April 04, 2024

Abstract

In recent years, there has been a shift towards using nonfullerene electron acceptors in organic solar cells (OSCs) as a replacement for fullerene derivatives. This change requires polymer donors that possess compatible physical properties, such as absorption range, HOMO energy level, miscibility, and crystallinity. Moreover, the high cost and poor batch-to-batch reproducibility of polymer donors also hinder future large-scale manufacturing. These emphasize the need to explore alternative types of polymer donors. The imide-functionalized building units possess several key attributes that make their polymers highly promising for non-fullerene OSCs. These attributes include ease of synthesis, strong electron-withdrawing ability, rigid and co-planar structure, and the ability to easily tune solubility through imide side chains. In this review, we summarized the synthetic routes of imide building units, and the structural evolution of imide-functionalized polymer donors by focusing on the effects of polymer structure on their physical, optoelectronic, and photovoltaic properties. We hope that this mini-review will serve as a catalyst for future research on imide-functionalized polymers toward high-performance, cost-effective, and durable organic solar cells (OSCs).

Cite this paper: *Chin. J. Chem.* **2023**, *41*, XXX—XXX.

DOI: 10.1002/cjoc.202300XXX

Recent advances of Imide-functionalized polymer Donors for Non-fullerene Solar Cells

Huijuan Wang,^{a,#} Songmin Mo,^{a,#} Dongyan Li,^a Qinghe Wu^{*,a}

^a Department of Chemistry and Key Laboratory for Preparation and Application of Ordered Structural Materials of Guangdong Shantou University Shantou, Guangdong 515063, China E-mail: wuqh@stu.edu.cn

Keywords

Imide | Polymer donors | Non-fullerene organic solar cells

Comprehensive Summary

In recent years, there has been a shift towards using nonfullerene electron acceptors in organic solar cells (OSCs) as a replacement for fullerene derivatives.

Huijuan Wang received her bachelor's degree from Nanyang Institute of Technology in 2021. Currently, she is a postgraduate student at Shantou University.
Songmin Mo got his B.S. degree from Guangzhou University in 2021. Now he is a master student at Shantou University.
Dongyan Li obtained her bachelor's degree from Shenzhen University in 2021. Now she is a master student at Shantou University.
Qinghe Wu received his B.S. degree (2007) in Chemistry from Henan University and Ph.D. degree (2013) in Organic Chemistry from Shantou University.
[#]These authors made equal contribution.

Contents

1. Introduction Page No.2
2. Imide-functionalized building units Page No.2
3. Imide-functionalized polymer donors Page No.2
 - 3.1. NTI-Based Polymers Page No.3
 - 3.2. TPD-based polymers Page No.5
 - 3.3. TzBI-based polymers Page No.8
 - 3.4. BTI-Based Polymers Page No.11
 - 3.5. PhI-based polymers Page No.12
 - 3.6. Other Imide-Based Polymers Page No.13
4. Conclusions and Outlook Page No.17

1. Introduction

In the past few years, the field of organic solar cells (OSCs) has experienced a significant increase in power conversion efficiency (PCE), surpassing 19 %, primarily due to the development of high-performance nonfullerene electron acceptors (NFAs).^[1-3] Zhan *et al.*, Zou *et al.* and Sun *et al.* made significant contributions by developing benchmark NFAs ITIC,^[4] Y6,^[5] and L8-BO.^[6] Compared with fullerene derivatives, these NFAs have different molecular geometry, strong absorption in the near-infrared (NIR) range, moderate HOMO energy levels, and high crystallinity.^[6-13] Because the photophysical properties and morphology compatibility between NFAs and polymer donors significantly affect photovoltaic performance of OSCs, these new NFAs demand matchable physical properties of polymer donors.^[12,14-19] Currently, the most widely used polymer donors are donor-acceptor (D-A) copolymers which were synthesized by coupling between electron-rich (D) and electron-deficient (A) units. Although several D-A polymer donors, such as PM6, D18, have shown a power conversion efficiency (PCE) over 19 %, ^[1,2,20,21] their high cost and poor batch-to-batch reproducibility highlight the importance to develop alternative types of polymer donors.^[22-24]

Among various of D-A copolymers, the imide-functionalized polymers have drawn considerable research attention and their use in organic field-effect transistor (OFET) and fullerene-based OSCs have been extensively explored.^[25-28] The imide building units have the following distinctive characteristics: 1) the strong electron-withdrawing ability of imide group could downshift the HOMO energy levels which benefit high V_{OC} values;^[29-31] 2) good π -conjugation of the planar core and interactions between O and other atoms are beneficial for intramolecular interaction and charge transport;^[22,32,33] 3) the N-alkyl side chain can adjust solubility and aggregation tendency of the polymer. Additionally, the N-alkyl chains, distant from the aromatic core, could minimize polymer chain π - π stacking and exert little influence on charge carrier mobility.^[34-37] 4) Last but not least, synthetic routes of most imide building units are straightforward from facile accessible materials.^[38,39] These advantages make imide-functionalized polymer donors really fascinating in nonfullerene OSCs.

Because the imide-functionalized polymers used in OFET and fullerene-based OSCs have been well summarized in previous comprehensive reviews,^[25,26,40] here, we focus especially on the recent advances of imide-functionalized polymer donors for non-fullerene OSCs. This review article first summarizes the latest structural evolution and common synthesis routes of classical imide-containing electron-deficient building blocks, then investigate the effects of polymer structure on their physical and optoelectronic properties, and introduce the application and photovoltaic performances of imide functionalized polymers in nonfullerene OSCs. In this review, the polymers were classified according to the types of imide-containing electron-deficient units,

and the emphasis on the relationships between the polymer structures, physical and photovoltaic properties will provide the guidelines on how to rationally design imide-functionalized polymer donors. It is hoped that this article provides ideas for future innovation on imide-functionalized polymers, especially towards high-performance, low-cost, and stable OSCs.

2. Imide-functionalized building units

The chemical structure, number of imide groups, and component of electron-deficient imide-functionalized building units significantly affect the photophysical and film-forming properties of their polymers, such as frontier energy levels, bandgap, absorption coefficient, crystallinity and charge transport.^[41-43] Historically speaking, the creation of new imide-functionalized unit played a crucial role in the evolution of imide-functionalized polymers. Till now, many imide building units have been created or developed, including naphthalene diimide (NDI),^[44] perylene diimide (PDI),^[26,45] thieno[3,4-c]pyrrole-4,6-dione (TPD),^[39,46,47] phthalimide (PHI),^[48,49] pyrrolo [3,4-*f*] benzotriazole-5,7(6*H*)-dione (TzBI),^[50,51] dithienophthalimide (DPI),^[35,52] naphthalenothiophene imide (NTI),^[22] bithiophene imide (BTI) units,^[53,54] naphthodithiophene imide (NDTI),^[55] thieno[3,4-*f*]isoindole-5,7-dione unit (TID),^[25,56] 5,9-di(thiophen-2-yl)-6*H*-pyrrolo[3,4-*g*]quinoxaline-6,8(7*H*)-dione (PQD),^[57,58] N-alkyl-4,7-di(thien-2-yl)-2,1,3-benzothiadiazole-5,6-dicarboxylic imide (DI),^[59,60] pyromellitic diimide (PMDI),^[61] tetraazabenzodifluoranthene diimide (BFI).^[62] The chemical structure of various imide-functionalized building units are illustrated in Figure 1. Due to strong electron-withdrawing ability, diimides building units are commonly employed in the construction of n-type semiconducting polymers for OFETs, as well as electron acceptors for OSCs, which have been well documented in other review articles.^[26,34] In this article, we aim to present the latest advancements in imide-functionalized polymer donors, categorizing them based on the specific types of imide units. The chemical structures of acceptor materials used below are shown in Figure 15.

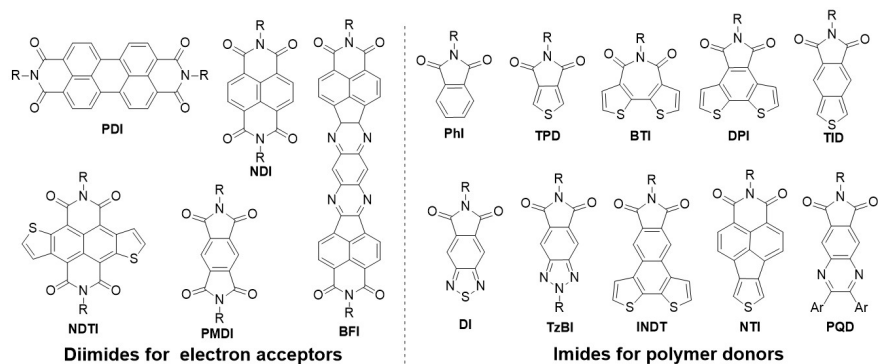


Figure 1 The chemical structure of various imide-functionalized building units.

3. Imide-functionalized polymer donors

3.1. Naphthalenothiophene Imide-Based Polymers

Scheme 1 Synthetic route of NTI and schematic reactions to form two Csp_2 - Csp_2 bonds by simple one-step reaction.

Six-membered imide has strong electron-withdrawing ability, and monomers with two six-membered imides, such as NDI and PDI, are widely used to construct n-type semiconducting materials for OFETs or electron acceptors for OSCs.^[63-65] However, the electron absorption ability of these diimides is too strong to be used as building units for polymer donors. Compounds with one six-membered will have weaker electron withdrawing ability and may be used as strong electron deficient monomers to construct polymer donors. Wu *et al.* reported the synthesis of naphthalenothiophene imide (NTI), which bears six-membered imide and a five-membered aromatic ring.^[22] The NTI compound was synthesized by Suzuki coupling between 6,7-dibromo-2-

(2-hexyldecyl)-1H-benzo[de]-isoquinoline-1,3(2-H)-dione and 3,4-bis(4,4,5,5-tetramethyl-1,3,2-dioxaborolan-2-yl)thiophene in a very high yield of 82 %. Notably, this is a new and efficient approach to construct five-membered aromatic ring, forming double $C_{sp2}-C_{sp2}$ bonds in a simple one-step reaction. The NDTI was also synthesized in a similar method from dibromo and ditin compounds. Because there are various dibromo and ditin/diBpin compounds, numerous fused-ring units for polymers could be created by using this method to form double $C_{sp2}-C_{sp2}$ bonds in a simple one-step reaction. The chemical structures of NTI-based conjugated polymers are illustrated in Figure 2 and the photovoltaic properties are summarized in Table 1.

Compared with other widely used electron-deficient units, such as BDD, TzBI, BTZ, the NTI has stronger electron-withdrawing ability and could significantly lower the HOMO energy levels of the polymers.^[15] Thus, the NTI-based polymer PNTB1 has a low-lying HOMO energy level (-5.42 eV) without introducing any F or Cl groups into the polymer backbone. The non-fullerene OSCs fabricated from PNTB1:Y6 exhibited the highest PCE of 15.18 %. They studied the impact of the thiophene π -bridge on photovoltaic performance through designing two NTI-based polymer donors PNTB and PNTB-2T.^[22] PNTB-2T has two more thiophene units in the polymer chain than PNTB, and exhibited better long-range coplanarity of polymer conjugated chains, resulting in closer π - π stacking, more ordered polymer chain packing, and higher hole transport of PNTB-2T. The PNTB-2T:Y6-based OSCs exhibited PCE of 16.72 %, while the PCE for PNTB:Y6 was only 3.81 %. The photovoltaic performance of PNTB-2T-based solar cells could be enhanced to 17.35 % by using PC₇₁BM as second acceptor. Importantly, NTI-based polymer donors exhibit excellent batch-to-batch reproducibility because the twisted polymer conjugated backbone make the polymer packed through weak short interactions rather than π - π stacking, which minimizes the impact of molecular weight on phase separation and blend film morphology.

Wu *et al.* also synthesized two NTI-based polymers PNTB6-Cl and PNTB-Cl by exploring the effect of employing linear or branched alkyl chains in NTI unit on photovoltaic performance.^[66] PNTB-Cl exhibited good solubility in chloroform, however, due to stronger intermolecular interactions and shorter π - π stacking distance, the polymer PNTB6-Cl with linear alkyl chains is insoluble in chloroform (Figure 3a, b). They fabricated layer-by-layer polymer solar cells (LBL-PSCs) with PNTB6-Cl as donor and N3 as acceptor by sequential spin-coating method (Figure 3c, d). Thus, PNTB6-Cl:N3 based LBL devices exhibited a remarkable PCE of 17.59 %, which is much higher than 15.24 % for PNTB-Cl:N3 based devices.

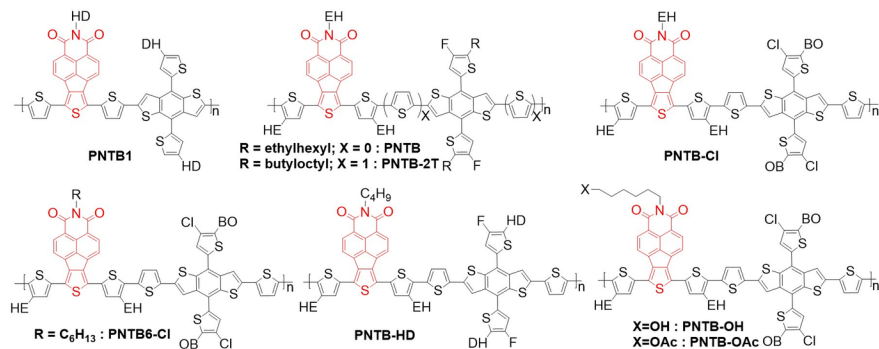


Figure 2 The chemical structures of NTI-based conjugated polymers.

Table 1 Summary of the photovoltaic properties of the polymer donors shown in Figure 2.

Donor	LUMO/HOMO [eV]	Acceptor	V_{OC} [V]	J_{SC} [mA cm ⁻²]	FF [%]	PCE [%]	Ref.
PNTB1	-3.51/-5.42	Y6	0.83	24.64	0.72	15.18	[15]
PNTB	-3.53/-5.60	Y6	0.90	8.68	49.0	3.81	[22]
PNTB-2T	-3.43/-5.52	Y6	0.87	26.31	73.0	16.72	[22]

Donor	LUMO/HOMO [eV]	Acceptor	V_{OC} [V]	J_{SC} [mA cm ⁻²]	FF [%]	PCE [%]	Ref.
PNTB-2T	—	Y6:PC ₇₁ BM	0.88	26.45	75.0	17.35	[22]
PNTB-Cl	-3.50/-5.49	N3	0.86	24.46	72.5	15.24	[66]
PNTB6-Cl	-3.49/-5.47	N3	0.86	26.58	77.3	17.59	[66]
PNTB6-Cl	—	Y6	0.88	26.63	74.83	17.53	[67]
PNTB6-Cl (BHJ)	—	BTP-4F-12	0.88	26.45	74.90	17.33	[68]
PNTB6-Cl (LBL)	—	BTP-4F-12	0.87	26.89	75.79	17.81	[68]
PNTB-HD	-3.53/-5.52	N3	0.85	26.88	79.0	18.15	[33]
PNTB-OH	-3.57/-5.33	N3	0.84	16.21	49.87	6.79	[69]
PNTB-OAc	-3.58/-5.41	N3	0.86	25.31	73.71	16.53	[69]
PNTB-HD	—	BTIC-OH- δ /N3	0.86	26.35	76.37	17.3	[70]

Importantly, three batches of PNTB6-Cl with varying molecular weights (Mn: 45.27-91.53 KDa) exhibited PCE deviation smaller than 4 %. It was further revealed that the chloroform processing dissolved the PNTB-Cl in both amorphous and crystalline regions, however, it only partially washed away amorphous PNTB6-Cl which bring forth the advantage of reducing the traps in LBL films that benefits the FF value, facilitating electron acceptor penetration. This study suggests the importance of controlling solubility properties of polymer donors toward high-performance LBL-OSCs. The use of different additives to control the donor and acceptor layers separately is a promising approach to achieve high efficiency of LbL-OSCs. Zhang *et al.* [67] prepared PNTB6-Cl:Y6-based LbL-OSCs by adding DPE and DFB solvent additives into PNTB6-Cl chlorobenzene solution and Y6 chloroform solution separately. It improves the photogenerated exciton distribution, charge transport and collection, resulting in PCE of 17.53 % that is much higher than 16.38 % for controlled devices. Using the same processing approach, they fabricated PNTB6-Cl: BTP-4F-12-based LbL-OSCs and achieved a PCE of 17.81 % by using DPE and DIO to optimize donor and acceptor layers separately.[68] Shao *et al.* [71] reported a self-powered organic photodetector (OPD) based on PNTB6-Cl:Y6 blend active film. The PNTB6-Cl:Y6 blend film exhibited a remarkable intrinsic stretchability up to 100 % strain. The OPD not only exhibited impressive weak-light detection ability, but also had a high anisotropic response rate of 1.42 under parallel and transversely polarized light irradiation.

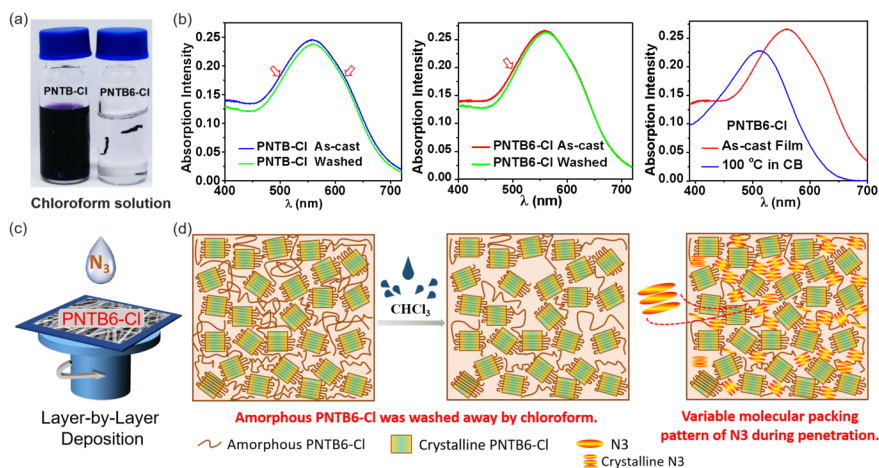


Figure 3 (a) Solubility of PNTB-Cl and PNTB6-Cl in chloroform after stirring for 24 h; (b) The absorption spectra of polymer pure films under different conditions (c) Schematics of LBL deposition; (d) Illustration of film morphology washed by chloroform and N₃ penetration between polymer domains. Reproduced with permission.^[16] Copyright 2021, The Royal Society of Chemistry.

Wu *et al.* [33] further developed a NTI-based polymer PNTB-HD by employing a linear chain in NTI. The PNTB-HD exhibited a stronger aggregation tendency in chloroform solution, which leads to higher hole mobility, better phase separation and favorable morphology of blend films. Therefore, the PNTB-HD:N3-based OSCs exhibited an optimized PCE of 18.15 %, which is much higher

than 16.77 % and 16.28 % for PNTB-2T:N3 and PM6:N3. Importantly, the PNTB-HD: N3 device also exhibited much better thermal stability with 82.9 % of initial efficiency maintained under continuous heating at 65 °C (Figure 4). The single crystal of NTIs with butyl and ethylhexyl substitutions provide some information to understand how the alkyl chains in NTI impact on physical properties of polymers. In NTI-EH, the distances of 2.72 and 2.67 Å between C=O and H-C were observed. However, interactions between C=O with H-C in NTI-Bu are much stronger and their distances of 2.49 and 2.55 Å are much shorter. He groups synthesized two polymers (PNTB-OAc and PNTB-OH) by introducing hydroxy (OH) or acetoxy (OAc) groups into the NTI unit.[69] Compared to the hydroxy group, the acetoxy group makes NTI-OAc have more regular hydrogen bonds and the polymer PNTB-OAc show ordered packing and stronger crystallinity. The PNTB-OAc:N3-based Q-PHJ OSCs achieved a much higher PCE of 16.53 %, while PCE for PNTB-OH is only 6.79 %. Additionally, the PNTB-OAc:N3-based Q-PHJ OSCs also deliver superior photostability and storage stability. He groups introduced a hydroxylated BTIC-OH- δ as a bifunctional layer in Q-PHJ film.[70] The inserted BTIC-OH- δ layer effectively protected the donor layer from the erosion of the chloroform solution, complemented the light absorption and formed cascade energy levels between the initial donor and an acceptor in a Q-PHJ device. The PNTB-HD: N3-based Q-PHJ OSCs treated with a BTIC-OH- δ molecular layer achieved a high PCE of 17.33 %, the corresponding semi-transparent device also achieved a PCE of 13.44 % with AVT of 23.62 %.

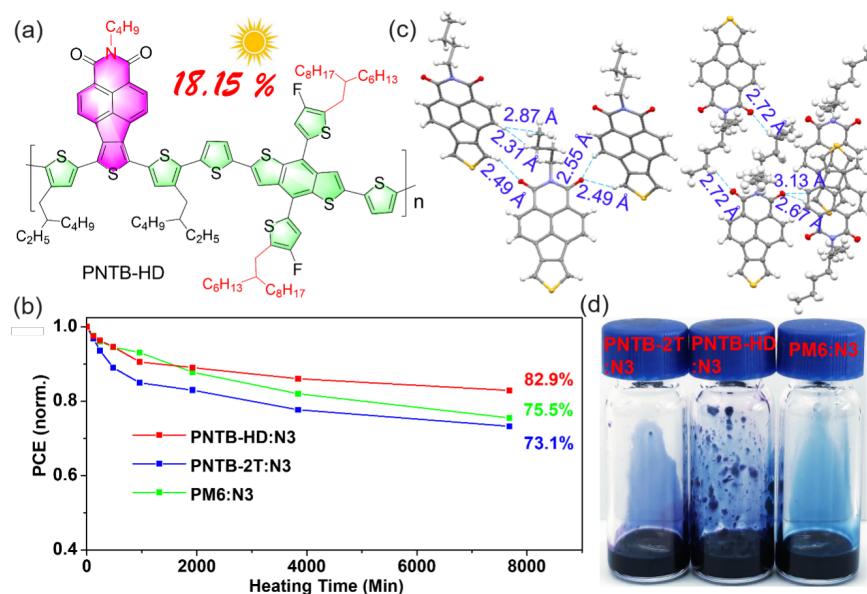


Figure 4 (a) Chemical structure; (b) Single-crystal data of NTI-EH and NTI-Bu; (c) Device thermal stability of polymers; (d) Aging of hot PNTB-HD:N3, PNTB-2T:N3 and PM6:N3 chloroform solution (identical with condition for device fabrication) for 2 h at room temperature. Reproduced with permission.[33] Copyright, 2022 Elsevier Ltd.

3.2. Thieno-[3,4-c]-pyrrole-4,6-dione (TPD) based polymers.

TPD unit was first synthesized by Sicé in 1954 by treating thiophene-3,4-dicarboxylic acid with ammonia.[72] Tour and co-workers first reported TPD-based conjugated copolymers in 1997.[73] TPD unit has the advantages of easy synthesis, high coplanarity, and strong electron-withdrawing ability.[46] In ad-

dition, Various side groups can be introduced into the N-site of TPD to tune solubility of the resulting polymer and morphology of blend films.^[39,46] To date, four synthetic routes have been reported for the preparation of TPD (Scheme 2) . Bjørnholm *et al.* ^[74] reported the synthesis of TPD from starting materials of 3, 4-dibromothiophene, which was converted to 3, 4-dicyanothiophene by Rosenmund-von Braun reaction with cuprous cyanide (Synthetic route 1). The alkaline hydrolysis of 3, 4-dicyanothiophene result in thiophenedicarboxylic acid, and then reflux in acetic anhydride to produce cyclic anhydride. The TPD was synthesized by treating 4-amino-thiophene-3-carboxylic acid with thionyl chloride. The synthesis of TPD dimer was based on the bromination of the TPD with 1 equiv of NBS, however, it makes the conditions hard to control to obtain the desired product with a good yield. In 2011, an efficient synthetic route was reported for the preparation of the 1-iodo-5-alkyl-4H-thieno[3,4-c] pyrrole-4,6(5H)-dione (TPD-I) by Leclerc *et al.* ^[75] They synthesized 3-ethyl 4-methyl 2-aminothiophene-3,4-dicarboxylate by the Gewald reaction between methyl 2-oxopropanoate and ethyl cyanoacetate. Then, the Sandmeyer-type reaction makes the amine of 3-ethyl 4-methyl 2-iodothiophene-3,4-dicarboxylate substituted by an iodide. Followed by acidic hydrolysis to obtain 3-ethyl 4-methyl 2-iodothiophene-3,4-dicarboxylate. Finally, 1-iodo-5-alkyl-4H-thieno[3,4-c]pyrrole-4,6(5H)-dione (TPD-I) was obtained via pyrroledione ring formation (Synthetic route 2). In 2015, Shinichiro Fuse *et al.* reported the synthesis of TPD through a Pd-catalyzed carbonylative amidation reaction from commercially available 3,4-dibromothiophene in a yield of 63 % (Synthetic route 3).^[76] It should be noted it is the most straightforward synthetic route to synthesize TPD by one-step reaction. In 2023, Min *et al.* reported a synthetic route of DT-TPD through a two-step reaction in a yield of 31 %.^[77] The key ring forming reaction was conducted by heating the mixture of 4-alkylthiophene-2-carbaldehyde, S8, 1-methylpyrrolidine-2,5-dione, 2-aminobenzimidazole, NH₄I, K₂CO₃, N-methyl-2-pyrrolidone and H₂O in 140 °C for 48 hours, yielding DT-TPD (Synthetic route 4).

Scheme 2 Synthetic route of TPD.

Leclerc *et al.* synthesized the a TPD-based polymer, and afforded a PCE of 5.5 % when blended with PC₇₁BM in 2010.^[78] After that, Thieno[3,4-c]pyrrole-4,6-dione (TPD) unit as an electron-deficient unit has been widely used to construct conjugated polymers for application in fullerene and non-fullerene based OSCs.^{[39,46],[79,80]} Figure 5 summarizes the structures of typical TPD-based polymers and relevant properties are listed in Table 2. Wang *et al.* ^[81] synthesized PBDT-TPD and PBDTS-TPD based on the BDT and TPD, and PCEs of 6.8 % and 7.7 % were achieved by blending with PNDI-T. Gao *et al.* ^[82] synthesized polymers PBDTT-TPD and PBDT-TPD. Compared with the alkoxy-modified polymer PBDT-TPD, the alkyl-thienyl modified polymer PBDTT-TPD possesses deeper HOMO energy level, higher extinction coefficient and better hole transport property, leading to a higher PCE of 7.15 % for PBDTT-TPD:IDIC based OSCs.

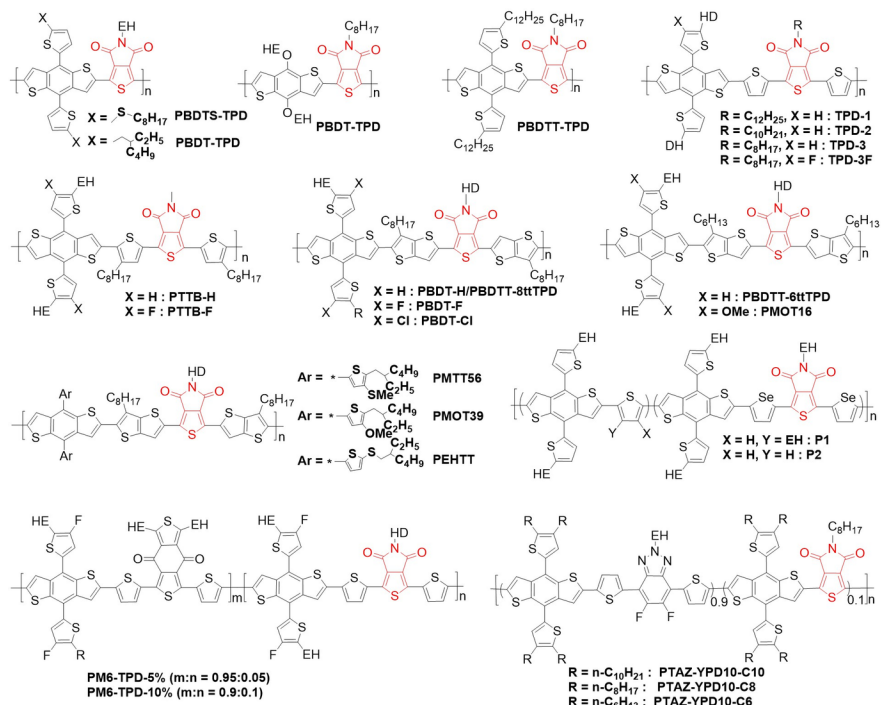


Figure 5 The chemical structures of TPD-based conjugated polymers.

Table 2 Summary of the photovoltaic properties of the polymer donors shown in Fig. 5.

Donor	LUMO/HOMO [eV]	Acceptor	V_{OC} [V]	J_{SC} [mA cm ⁻²]	FF [%]	PCE [%]	Re
PBDT-TPD	-3.77/-6.09	PNDI-T	1.10	10.8	57.0	6.8	[81]
PBDTS-TPD	-3.84/-6.12	PNDI-T	1.10	11.5	61.0	7.7	[81]
PBDT-TPD	-3.06/-5.36	ITIC	0.88	10.13	48.7	4.36	[82]
PBDTT-TPD	-3.09/-5.51	IDIC	0.90	14.31	55.5	7.15	[82]
TPD-3	-3.59/-5.49	IT-4F	0.80	20.1	75.3	12.1	[88]
TPD-3F	-3.73/-5.62	IT-4F	0.91	20.5	73.8	13.8	[88]
TPD-3	—	Y6	0.83	26.70	68.5	15.2	[89]
TPD-3F	—	Y6	0.87	21.07	62.2	11.4	[89]
PTTB-H	-3.46/-5.33	L8-BO	0.83	24.5	65.9	13.3	[77]
PTTB-F	-3.70/-5.6	L8-BO	0.88	26.6	77.1	18.1	[77]
PBDTT-6ttTPD	-3.51/-5.36	IDIC	0.82	15.9	65.5	8.6	[47]
PMOT16	-3.66/-5.52	IDIC	0.93	16.1	67.3	10.0	[47]
PBDT-H	-3.48/-5.35	Y6	0.74	24.9	63.0	11.6	[90]
PBDT-F	-3.64/-5.51	Y6	0.83	25.4	68.0	14.4	[90]
PBDT-Cl	-3.64/-5.53	Y6	0.85	25.7	71.0	15.4	[90]
PBDTT-8ttTPD-L	-3.37/-5.23	ITIC	0.92	10.9	53.0	5.3	[91]
PBDTT-8ttTPD-M	—	ITIC	0.91	14.9	58.0	7.9	[91]
PBDTT-8ttTPD-H	—	ITIC	0.93	17.1	68.0	10.8	[91]
PMTT56	-3.40/-5.39	IT-2F	0.95	18.7	71.4	12.6	[92]
PMOT39	-3.38/-5.34	IT-2F	0.90	17.8	65.8	10.5	[92]
PEHTT	-3.39/-5.35	IT-2F	0.89	18.9	64.4	10.8	[92]
PM6-TPD-5 %	-3.74/-5.54	Y6	0.86	25.12	75.3	16.3	[93]
PM6-TPD-10 %	-3.73/-5.57	Y6	0.85	23.68	73.0	14.8	[93]

Donor	LUMO/HOMO [eV]	Acceptor	V_{OC} [V]	J_{SC} [mA cm ⁻²]	FF [%]	PCE [%]	Re
PM6:PM6-TPD-5 %	—	Y6	0.86	26.07	76.2	17.1	[93]
PTAZ-TPD10-C10	-3.24/-5.27	N2200	0.87	11.2	70.0	6.8	[94]
PTAZ-TPD10-C10	—	ITIC	0.91	14.7	66.0	8.8	[94]
PTAZ-TPD10-C8	-3.23/-5.27	N2200	0.88	9.4	60.0	5.0	[94]
PTAZ-TPD10-C8	—	ITIC	0.89	12.6	60.0	6.7	[94]
PTAZ-TPD10-C6	-3.23/-5.26	N2200	0.86	4.4	60.0	2.3	[94]
PTAZ-TPD10-C6	—	ITIC	0.86	10.6	60.0	5.5	[94]
P1	-3.52/-5.38	ITIC	0.86	18.5	50.1	7.9	[95]
P2	-3.69/-5.43	ITIC	0.83	6.31	37.4	2.0	[95]

The thiophene, thieno[3,2-*b*]thiophene, selenophene, and furan moieties have been widely used as π -bridges to tune TPD-based polymers' photophysical and photovoltaic properties.^[83-87] Facchetti *et al.* reported a series of polymers TPD-1-3, and explored the effects of alkyl side chain length and fluorine atom substitutions on physical properties of TPD-based polymers.^[88] The TPD-1-3 exhibited good solubilities, high hole transport, and matched frontier energy levels with IT-F4. The efficiency of the devices decreases as the chain length increase, and the efficiency of 11.7 %, 11.8 % and 12.1 % were obtained for TPD-1, TPD-2 and TPD-3-based PSCs by using *o*-xylene solvent. The presence of the F atom on the BDT deepens the HOMO energy level, resulting in TPD-3F: IT-4F based OSC with a PCE of 13.8 % and a high V_{OC} 0.91eV. However, by matching with non-fullerene acceptor Y6, the TPD-3 exhibited an PCE of 15.2 %, while that for TPD-3F is 11.4 % probably due to the mismatch of HOMO energy level.^[89] Recently, Min *et al.* designed a TPD-based polymer donor PTTB-F, which showed an decent PCE of 18.06 % in binary OSCs by blending with L8-BO.^[77] By employing thieno[3,2-*b*]thiophene as the π -bridge, Liang *et al.* synthesized TPD-based polymers PBDTT-6ttTPD and PMOT16.^[47] By blending with IDIC, the PMOT16-based OSCs exhibited a PCE of 10.04 %. Later, they synthesized polymers PMTT56, PMOT39 and PEHTT by introducing different side chains in BDT unit.^[92] By matching with IT-2F, PMTT56, PMOT39 and PEHTT based OSCs achieved the highest PCEs of 12.6 %, 10.5 % and 10.8 %, respectively. It should be noted that the high PCEs were obtained by using non-halogenated solvent toluene. By adding PC₇₁BM as the second acceptor, the PCE of PMTT56-based ternary devices was further enhanced to 13.2 %. Later, Kim *et al.* developed three polymers PBDT-H, PBDT-F and PBDT-Cl based on thienothiophene π -bridged *N*-octylthieno[3,4-*c*]pyrrole-4,6-dione (8ttTPD) and benzo[1,2-*b*:4,5-*b'*] dithiophene (BDT) units.^[90] They found that the incorporation of highly planar structured 8ttTPD unit could improve crystallinity and hole mobilities of the BDT-based polymers. Besides, the introduction of the halogen atoms on BDT unit could tune the crystallinity and energy levels. Synergistic effects of incorporated 8ttTPD unit and halogen atoms could significantly facilitate the charge transporting properties and charge recombination process, which is stemmed from the enhanced crystallinity and hole mobility of the polymers. Therefore, the PBDT-Cl:Y6-based OSCs achieved the highest PCE of 15.63 %, which out-performs the 11.84 % for PBDT-H:Y6 and 14.86 % for PBDT-F:Y6. To investigate the effect of molecular weight on the photovoltaic performances, Hwang *et al.*^[91] synthesized three batches of PBDTT-8ttTPD with different molecular weights. The higher molecular weight could improve the ordering of polymer packing, π - π stacking distance, absorption coefficient, and nanomorphology of the blend films. The batch with highest molecular weight demonstrates the highest PCE of 11.05 %, which is much higher than 8.27 % and 5.34 % for the batches with the medium and lowest molecular weight.

By introducing the third unit (D2 or A2) into the D-A copolymer, the random terpolymer strategy have been proved to be an efficient method to fine-tune the frontier energy levels, optical properties, and film-forming properties of the polymer.^[83,96,97] The TPD unit was also broadly used to in terpolymers. Chen and coworkers designed and synthesized a D-A1-D-A2-type terpolymer (PM6-TPD-5 %) via random copolymerization.^[93] The addition of TPD results in polymers with lower HOMO, wider light absorption, optimal molecular packing, and more ideal morphology of blend film. PM6-TPD-5 %: Y6-based binary organic solar cells showed an encouraging PCE of 16.3 %, which out-performs the 14.8 % for PM6-TPD-10 %: Y6 and 15.6 % for PM6: Y6. Besides, a PCE of 17.1 % was obtained in PM6: PM6-TPD-5 %: Y6 based ternary

OSCs. Cao *et al.* synthesized a set of random terpolymers PTAZ-TPD10- C_n , which are composed of an electron-rich unit BDT, and two electron-deficient units of TAZ and TPD.^[94] The PCE of the N2200 and ITIC-based devices decreases monotonically when shortening the side chain of PTAZ-TPD10- C_n from decyl to hexyl. However, the PCEs of PTAZ-TPD10- C_n :PC₆₁BM-based OSCs increase monotonically. Toppare and coworkers synthesized two random copolymers P1 and P2 by using benzodithiophene (BDT) and thiophenes as donor moiety, TPD as acceptor, and selenophene as π -bridging unit.^[95] Compared with polymer P2, P1 containing alkyl thiophene have a larger molecular weight and better solubility, resulting in a higher PCE of 7.94 % for P1: ITIC which is much higher than 1.96 % for P2: ITIC.

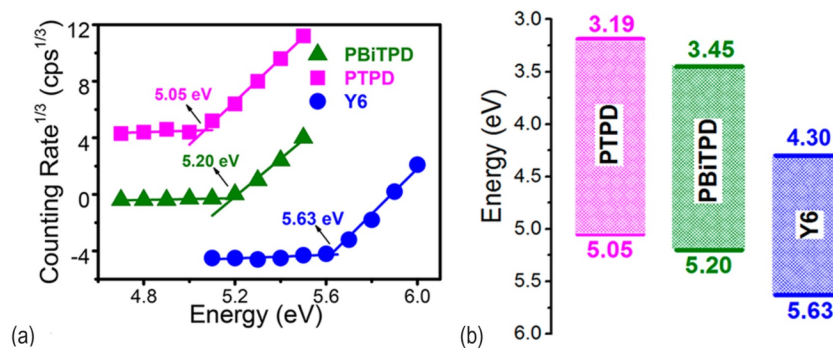


Figure 6 (a) Photoelectron spectroscopy in air (PESA) curves for PTPD, PBiTPD, and Y6. PESA-inferred IPs are reported on the plots, and the traces are offset for clarity. (b) Energy level alignments (IP and EA) of electron acceptor Y6 and electron donors PTPD and PBiTPD. Reproduced with permission.^[98] Copyright 2020, American Chemical Society.

As a derivative of TPD, Bi-thieno[3,4-c]pyrrole-4,6-dione (bi-TDP) has a larger planar backbone and much stronger electron-withdrawing ability, which make it a promising electron-deficient units for polymer semiconductors.^[28,39,46,99,100] Its application in polymer donors was also investigated. The chemical structures of biTPD-based polymer donors are illustrated in Figure 7 and the photovoltaic properties are summarized in Table 3. Huang and coworkers synthesized two polymer donors PBiTPD and PTPD.^[98] The biTPD-based polymer PBiTPD has a larger ionization potential (IP) value (ca. 5.20 eV) than PTPD (ca. 5.05 eV), which leads to a higher V_{OC} values of the donor polymer PBiTPD in BHJ solar cells (Figure 6a). The first-level electron affinity (EA) values were 3.19 eV for PTPD, 3.45 eV for PBiTPD, and 4.30 eV for Y6 (Figure 6b), respectively. In addition, the GIWAXS results indicate that PBiTPD and PBiTPD: Y6 BHJ blend films exhibited more favorable face-on backbone orientation and stronger crystallinity. Therefore, the PBiTPD:Y6-based OSCs exhibited a PCE of 14.2 % that is much higher than 5.9 % for PTPD:Y6-based devices.

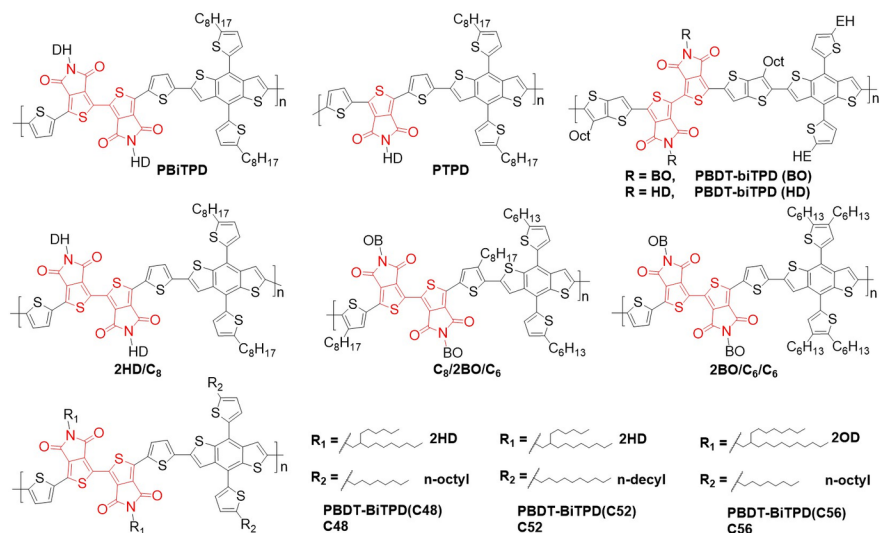


Figure 7 The chemical structures of bi-TPD-based conjugated polymers.

Table 3 Summary of the photovoltaic properties of the polymer donors shown in Figure 7.

Donor	LUMO/HOMO [eV]	Acceptor	V_{OC} [V]	J_{SC} [mA cm^{-2}]	FF [%]	PCE [%]	Ref
PTPD	-3.19/-5.05	Y6	0.66	19.5	46.0	5.9	[98]
PBiTPD	-3.45/-5.80	Y6	0.83	25.6	66.7	14.2	[98]
PBDT-BiTPD(C48)	—	Y6	0.82	25.9	66.5	14.0	[101]
PBDT-BiTPD(C52)	—	Y6	0.81	23.7	58.3	11.0	[101]
PBDT-BiTPD(C56)	—	Y6	0.80	20.9	47.3	7.6	[101]
2HD/C8	-2.85/-5.08	Y6	0.83	25.6	66.8	14.0	[102]
C8/2BO/C6	-2.78/-5.00	Y6	0.79	9.6	31.1	2.2	[102]
2BO/C6/C6	-2.85/-5.05	Y6	0.86	21.1	48.0	8.5	[102]
PBDT-biTPD(BO)	-3.52/-5.33	PC ₇₁ BM	0.89	13.2	71.4	8.5	[31]
PBDT-biTPD(BO)	—	IT-4F	0.82	17.1	66.3	9.3	[31]
PBDT-biTPD(HD)	-3.54/-5.38	PC ₇₁ BM	0.91	13.4	73.5	9.0	[31]
PBDT-biTPD(HD)	—	IT-4F	0.85	16.6	67.0	9.5	[31]

Later, the effect of alkyl chains on optical and photovoltaic properties was further studied.^[101] The GIWAXS test results indicate that as the alkyl side chain length decreases from C56 to C48, the crystal surface orientation and molecular order increases significantly. As a result, PBDT-BiTPD-C48 with the shortest alkyl side chains achieved the best photovoltaic performance with the PCE of 14.1 %, while that for other two polymers (C52 and C56) are 11.1 % and 7.8 %, respectively. Cai *et al.*^[102] synthesized three polymers 2HD/C8, C8/2BO/C6, and 2BO/C6/C6 by introducing side alkyl chains into different positions. Introducing alkyl side chains to the thiophene (T) motifs in C8/2BO/C6 or to the BDT motifs in 2BO/C6/C6 decrease the crystallinity and face-on crystallite orientation, resulting in serious charge recombination loss and decreased FF and J_{SC} in BHJ devices. Hwang *et al.*^[31] synthesized two biTPD-based polymers PBDT-biTPD(BO) and PBDT-biTPD(HD) with different lengths of the alkyl side chain. Due to the strong electron-withdrawing strength of biTPD, both polymers show deeper HOMO and LUMO energy levels than those for TPD-based polymers. By blending with IT-4F, PBDT-biTPD(BO) and PBDT-biTPD(HD)-based OSCs showed the PCE of 9.49 % and 9.32 %, respectively.

3.3. TzBI-Based Polymers.

Scheme 3 Synthetic Route to TzBI

The imide-functionalized benzotriazole (TzBI) unit was firstly reported by Huang *et al* ^[51]. The Diels-Alder reaction of 1, 3-di-2-thienothiophene [3,4-c][1,2,5] thiadiazole-2-S (IV) (1) with dimethyl acetylenedicarboxylate yield 4,7-Di(thien-2-yl)-2,1,3-benzothiadiazole-5,6-Dicarboxylate (2). Followed by alkaline hydrolysis, anhydride and imide formation, N-alkyl-4,7-di(thien-2-yl)-2,1,3- benzothiadiazole-5,6-dicarboxylic imide (5) was prepared accordingly. The reduction reaction of compound 5 by iron powder, the cyclization reaction with excess NaNO₂ and condensation reaction with amine give the compound 4,8-di(thien-2-yl)-6-octyl-2-octyl-5*H*- pyrrolo[3,4-*f*]benzotriazole-5,7(6*H*)-dione (TzBI) successfully (Scheme 3). Presented in Figure 8 are the chemical structures of some TzBI-based polymers and their corresponding photophysical properties and photovoltaic performance are summarized in Table 4. They synthesized TzBI-based WBG polymer PTZBIBDT by coupling with BDT unit.^[51] The PTZBIBDT:PC₇₁BM OSCs exhibited a PCE of 8.63 %. By blending with a high molecular weight polymer acceptor N2200, the PTzBI:N2200-based all-PSC devices exhibited a high PCE of 9.16 %. It should be noted that this efficiency was obtained from the OSCs that was prepared from the environmentally friendly solvent MeTHF.^[103] They also synthesized a wide-bandgap polymer PTzBI-DT by coupling with DTBDT unit.^[104] Devices based on PTzBI:ITIC and PTzBI-DT:ITIC achieved PCEs of 10.24 % and 9.43 %, respectively.

Incorporating appropriate side chains into the TzBI groups can affect the optoelectronic properties of polymers. Huang *et al.* ^[105] synthesized a polymer PTzBI-O, by replacing the alkyl side chain in TzBI with a polar substituent. The addition of oxygen atom enhanced the electron-withdrawing ability of theTzBI, resulting in a red-shifted absorption and strong preaggregation of PTzBI-O. A PCE of 7.9 % was achieved for PTzBI-O:N2200 based all-PSC devices. They further synthesized a copolymers PTzBI-Si that has a siloxane-terminated side-chain in TzBI.^[106] Because the siloxane-functionalized side chains endow PTzBI-Si with excellent solubility in the green-solvent MeTHF, the photovoltaic performance of PTzBI-Si:N2200-based OSCs processed from green-solvent MeTHF was improved to 10.24 %. The increased the molecular weight of PTzBI-Si could optimize the morphology of the active layer,^[107] leading to a PCE of 11.5 % in PTzBI-Si:N2200-based devices.

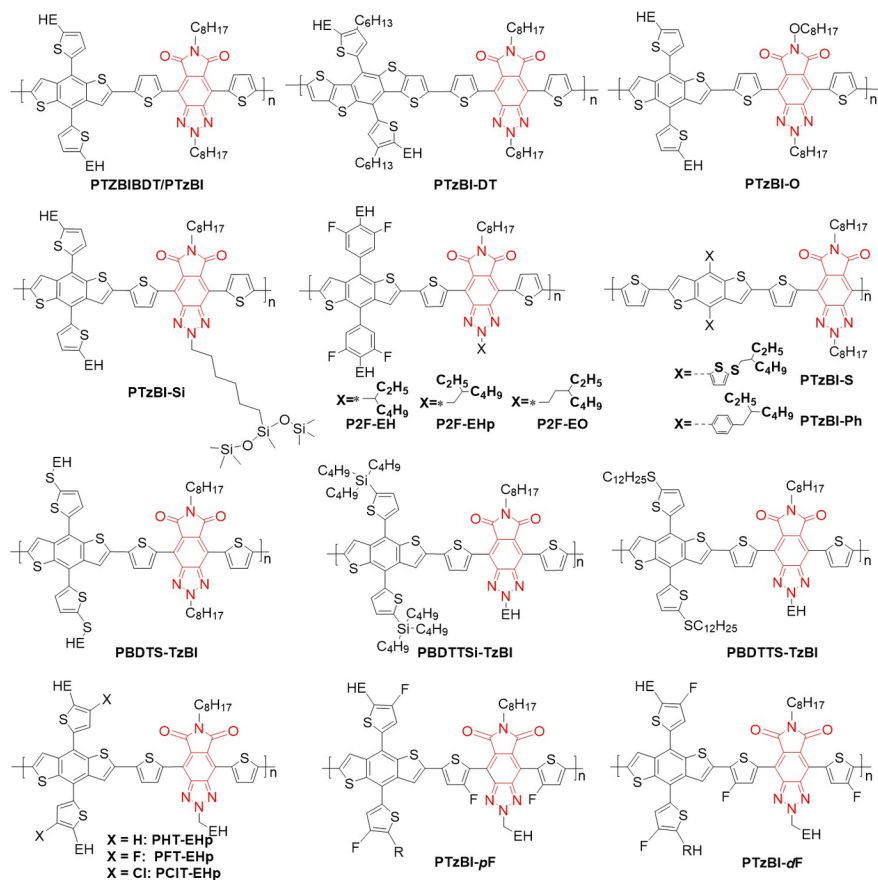


Figure 8 The chemical structures of TzBI-based conjugated polymers.

Table 4 Summary of the photovoltaic properties of the polymer donors shown in Figure 8.

Donor	LUMO/HOMO [eV]	Acceptor	V_{OC} [V]	J_{SC} [mA cm^{-2}]	FF [%]	PCE [%]	Ref.
PTZBIBDT	-3.46/-5.34	N2200	0.87	13.50	73.95	8.63	[51]
PTzBI	—	N2200 _{HW}	0.86	14.84	62.20	8.06	[103]
PTzBI	—	N2200 _{MW}	0.85	11.48	57.17	5.67	[103]
PTzBI	—	N2200 _{LW}	0.85	10.39	51.98	4.86	[103]
PTzBI-DT	-3.51/-5.39	ITIC	0.91	16.84	61.53	9.43	[104]
PTzBI	-3.46/-5.34	ITIC	0.87	18.29	64.34	10.24	[104]
PTzBI-O	-3.44/-5.44	N2200	0.86	14.70	63.98	7.91	[105]
PTzBI-Si	-3.10/-5.31	N2200	0.87	15.74	73.98	10.1	[106]
PTzBI-Si _L	—	N2200	0.86	14.1	72.7	8.6	[107]
PTzBI-Si _H	—	N2200	0.86	17.5	78.6	11.5	[107]
P2F-EHp	-3.06/-5.38	IT-2F	0.85	24.8	72.1	15.2	[108]
P2F-EHp	-3.13/-5.46	BTPT-4F	0.78	3.20	43.78	1.09	[109]
P2F-EHp	—	BTPTT-4F	0.81	26.68	74.11	16.02	[109]
PTzBI-S	-3.54/-5.38	ITIC	0.92	16.62	60.01	9.12	[110]
PTzBI-Ph	-3.58/-5.43	ITIC	0.82	16.39	67.72	10.19	[110]
PBDTS-TzBI	-3.52/-5.39	ITIC	0.94	17.01	56.79	9.04	[50]

Donor	LUMO/HOMO [eV]	Acceptor	V_{OC} [V]	J_{SC} [mA cm^{-2}]	FF [%]	PCE [%]	Ref.
PBDTS-TzBI	—	ITIC-Th	0.92	17.66	62.36	9.67	[50]
PBDTTSi-TzBI	-3.08/-5.46	ITIC	0.98	12.70	55.0	6.85	[111]
PBDTTS-TzBI	-3.32/-5.38	ITIC	0.85	16.36	69.0	9.60	[111]
PCIT-EHp	—	Y6	0.80	27.3	72.6	15.8	[112]
PCIT-EHp	—	Y6DT	0.84	25.8	75.8	16.4	[112]
PTzBI-pF	-3.83/-5.55	Y6	0.80	4.88	36.5	1.4	[113]
PTzBI-dF	-3.58/-5.67	Y6	0.85	26.33	75.5	16.8	[113]
PTzBI-dF	—	L8BO	0.88	24.51	76.49	16.74	[114]
PTzBI-dF	—	L8BO:Y6	0.86	26.95	78.78	18.26	[114]

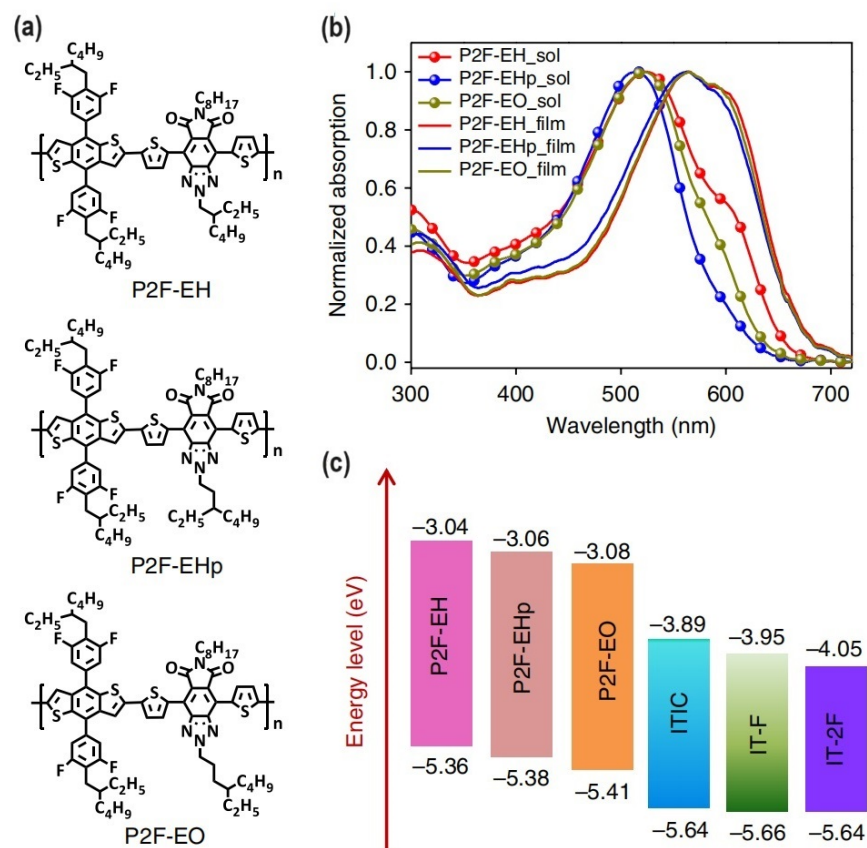


Figure 9 (a) Chemical structures of the donor polymers (b) Normalized ultraviolet–visible absorption of the donor polymers in dilute chloroform solution and as neat films. (c) Energy level diagram of thin films obtained from cyclic voltammety measurements. Reproduced with permission.^[108] Copyright 2018, Springer Nature Limited.

By fine-tuning the number of carbon atoms connected to the branched alkyl group in TzBI unit, they synthesized a series of polymer, termed P2F-EH, P2F-EHp and P2F-EO, respectively.^[108] As branching point was moved away conjugated core, the HOMO energy level of the polymers is consistently lowered (P2F-EH, -5.36 eV; P2F-EHp, -5.38 eV; P2F-EO, -5.41 eV). The energy levels of the materials are illustrated in Figure 9. The P2F-EHp has the best photovoltaic performance (7.28 %), which is higher than 6.13 % for

P2F-EH: ITIC and 6.73 % for P2F-EO: ITIC. By blending with IT-2F, the P2F-EHp:IT-2F device exhibited an optimized PCE of 12.11 %. By paring with BTPPT-4F and finely optimizing the morphology of the blend film, P2F-EHp: BTPPT-4F displayed a PEC over 16 %.^[109]

The polymer PTzBI-S and PTzBI-Ph with an alkylthiothienyl or alkylphenyl chain on the BDT unit were also synthesized.^[110] The PTzBI-S:ITIC and PTzBI-Ph:ITIC showed PCEs of 9.12 % and 10.19 %, respectively. Zhang *et al.*^[50] synthesized polymer PBDTS-TzBI that have a PCE of 9.04 % with a high V_{OC} of 0.94 V without using any processing additive when blending with ITIC. Negash *et al.*^[111] synthesized PBDTTSi-TzBI and PBDTTS-TzBI by replacing the alkyl side chain with the alkyl silyl or alkylthio side chains in BDT. A PCE of 9.6 % was obtained for PBDTTS-TzBI:ITIC based devices.

Li *et al.*^[112] synthesized three TzBI-based polymers, namely, PHT-EHp, PFT-EHp and PCIT-EHp. Owing to the strong electron-withdrawing ability of both imide group and halogen atoms, the polymers substitutions exhibited slight blue-shift absorption and deepened HOMO levels (-5.60 eV, -5.64 eV, and -5.71 eV, respectively). By blending with ITIC, the PCIT-EHp showed a high PCE of 15.8 % that is higher than 7.7 % for PHT-EHp and 15.4 % for PFT-EHp. Additionally, the PCIT-EHp:Y6DT-based binary devices demonstrated an efficiency 16.4 %. To explore the impact of the fluorine substitution points on thiophene π -bridge on photovoltaic performance, Huang *et al.*^[113] synthesized PTzBI-*p* F and PTzBI-*d* F. The PTzBI-*d* F has a more planar molecular conformation, narrower bandgap, and higher hole mobility. The PTzBI-*d* F: Y6-based device has an optimized PCE of 16.8 %, which is much higher than 1.4 % for PTzBI-*p* F: Y6. Using L8-BO as the second acceptor,^[114] the PTzBI-*d* F:L8-BO:Y6 ternary devices exhibited a promising PCE of 18.26 % and excellent long-term thermal stability under 85 °C.

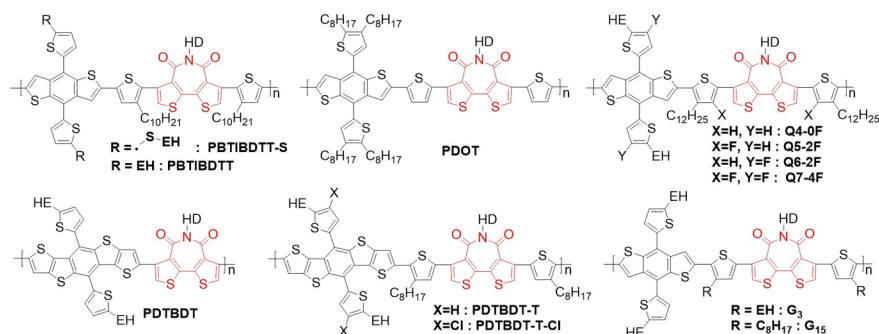


Figure 10 The chemical structures of BTI-based conjugated polymers.

Table 5 Summary of the photovoltaic properties of the polymer donors shown in Figure 10.

Donor	LUMO/HOMO [eV]	Acceptor	V_{OC} [V]	J_{SC} [mA cm ⁻²]	FF [%]	PCE [%]	Ref.
PBTIBDTT	-3.60/-5.47	PC ₇₁ BM	0.91	14.53	71.29	9.42	[117]
PBTIBDTT-S	-2.85/-5.53	PC ₇₁ BM	0.96	11.98	69.76	8.02	[117]
PBTIBDTT	—	ITIC-F	0.92	16.40	74.1	11.19	[118]
PDOT	-3.58/-5.50	PC ₇₁ BM:ITIC	0.96	17.49	66.8	11.21	[119]
PDTBDT	-3.28/-5.67	Y6	0.90	17.18	53.50	8.22	[115]
PDTBDT-T	-3.21/-5.40	Y6	0.78	24.21	65.81	12.71	[115]
PDTBDT-T-Cl	-3.26/-5.58	Y6	0.86	24.49	71.65	15.63	[115]
Q4	-3.63/-5.52	MeIC	0.99	13.57	76.90	10.34	[120]
Q5	-3.79/-5.74	MeIC	1.08	13.59	74.90	11.06	[120]
Q6	-3.81/-5.70	MeIC	1.11	7.50	63.00	5.26	[120]
Q7	-3.82/-5.78	MeIC	1.09	1.15	38.50	0.48	[120]
Q4	—	PYIT	0.94	21.59	73.90	15.06	[120]
G3	—	L15	0.97	7.08	55.89	3.82	[121]

Donor	LUMO/HOMO [eV]	Acceptor	V_{OC} [V]	J_{SC} [mA cm ⁻²]	FF [%]	PCE [%]	Ref.
G15	—	L15	0.93	22.87	70.98	15.17	[121]

3.4. Bithiopheneimide (BTI)-Based Polymers

Scheme 4 Synthetic Route to Bithiopheneimide (BTI)

Bithiophene imide (BTI) unit with seven-membered imide ring was first designed and synthesized by Marks and coworkers in 2008.^[36] The reduction reaction of 3,3',5,5'-tetrabromo-2,2'-bithiophene with zinc powder yields 3,3'-dibromo-2,2'-bithiophene. 2,2'-bithiophene-3,3'-dicarboxylic acid was prepared by adding n-BuLi and then treating with carbon dioxide gas. Through condensation cyclization in acetic anhydride and substitution reaction with amine, BTI was successfully synthesized (Scheme 4). The BTI unit shows a strong electron withdrawing ability to reduce the highest occupied molecular orbital (HOMO) level and a good planarity to reduce the steric hindrance effectively.^[53,115] The first BTI-based polymer P2 for OPV application exhibited a PCE of 5.5 % when blend with PC₇₁BM.^[116] After that, the development of BTI-polymers for OSCs had gained much attention. The chemical structures of BTI-based polymer donors are illustrated in Figure 10 and the photovoltaic properties are summarized in Table 5.

Yang *et al.*^[117] synthesized polymers PBTIBDTT and PBTIBDTT-S and realized high PCEs of 8.6 % and 9.42 % by blending with PC₇₁BM.

The PCEs could remain above 8.6 % as the active layer thickness further increased to 280 nm. By matching with the ITIC-F, PBTIBDTT-based PSCs showed an outstanding PCE of 11.2 %.^[118] Notably, A PCE over 9 % can be maintained when the active layer thickness reached 350 nm, suggesting that PBTIBDTT-based devices are insensitive to the active layer thickness. They also reported a ternary OSC using PDOT as the donor polymer and PC₇₁BM and ITIC as co-acceptors.^[119] By finely controlling the morphology via the ratio control of ternary blends, a PCE of 11.21 % was achieved in ternary OSC. Wei *et al.* reported three BTI-based polymers (PDTBDT, PDTBDT-T, and PDTBDT-T-Cl) by introduced thiophene π -bridges and chlorine atoms to optimized light absorption and the energy level of the polymers.^[115] The HOMO and LUMO energy levels were -5.67 and -3.28 eV for PDTBDT, -5.40 and -3.21 eV for PDTBDT-T, and -5.58 and -3.26 eV for PDTBDT-T-Cl, respectively. The optimized PDTBDT-T-Cl:Y6 OSCs achieved a PCE of 15.63 %, which is much higher than 12.71 % for PDTBDT-T:Y6 and 8.22 % for PDTBDT:Y6.

Yan *et al.* reported four BTI-based polymers, Q4, Q5, Q6, and Q7.^[120] Blending with MeIC, the devices based on Q4, Q5, Q6, and Q7 showed PCEs of 10.34, 11.06, 5.26, and 0.48 %, respectively. Due to suitable energy levels and complementary optical absorption with PYIT, Q4: PYIT based all-PSCs achieved the highest PCE of 15.06 %, while the other three polymers (Q5-Q7) exhibited much lower PCEs in the range of 0.12-6.71 %. Recently, Guo *et al.* synthesized two BTI-based polymers that have the same backbone but isomeric alkyl side-chains on thiophene π -bridge.^[121] The isomerization of alkyl chains significantly affected their crystallinity and molecular orientation behaviors. G15 with linear octyl side-chains on thiophene π -bridges features more planar backbone, stronger pre-aggregation character in solution and distinctive temperature-dependent aggregation (TDA) property. As a result, G15-based all-polymer OSCs yielded a high PCE of 15.17 %, which is much higher than 3.82 % for G3:L15-based devices.

3.5. Phthalimide (PhI) based polymers

Scheme 5 Synthetic Route to Phthalimide (PhI).

Watson *et al.* reported the synthesis of PhI-2Br from starting materials phthalic anhydride, which converted to 4, 7-dibromoisobenzofuran-1,3-dione in presence of Br₂ in fuming sulfuric acid solution, followed by treating with amines in glacial acetic acid.^[122] The synthetic route to Phthalimide (PhI) is depicted in Scheme 5. The PhI unit was firstly introduced into polymers for optoelectronic devices by Guo and co-workers in 2009.^[48] The first PhI-based polymer poly(N-(dodecyl)-3,6-bis(4-dodecyloxy-thiophen-2-yl))phthalimide (PhIBT12) exhibited a relatively low PCE of 1.92 % by blending with PC₆₁BM.^[123] The PhI-based polymers have very

wide bandgap and the highest PCEs were only 6.3 % by matching with fullerene acceptors.^[124,125] However, PhI-based polymers demonstrated much better photovoltaic performance by matching with narrow bandgap NFAs. The chemical structures of PhI-based polymer donors are illustrated in Figure 11 and the photovoltaic properties are summarized in Table 6.

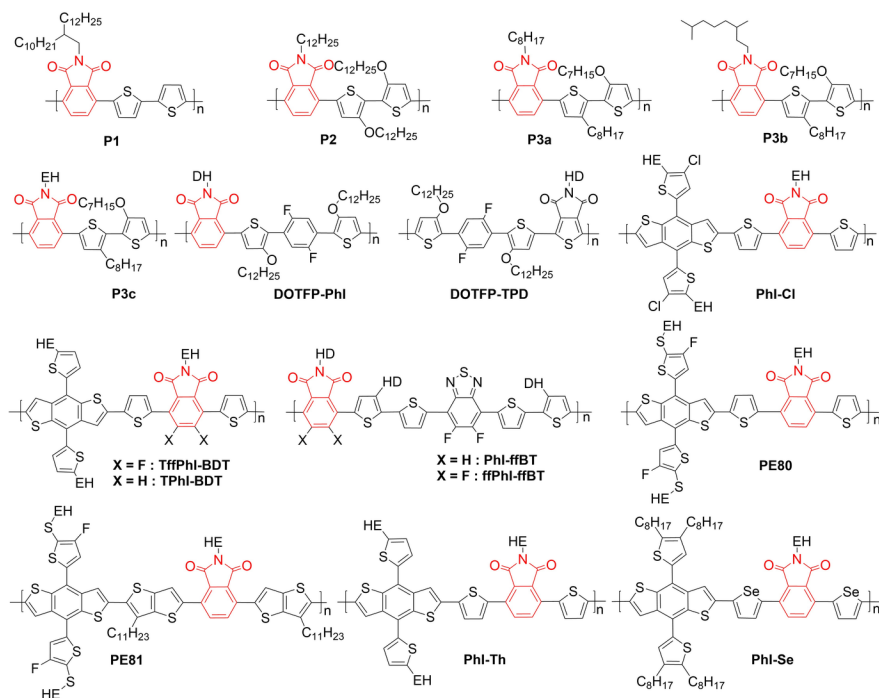


Figure 11 The chemical structures of PhI -based conjugated polymers.

Table 6 Summary of the photovoltaic properties of the polymer donors shown in Figure 11.

Donor	LUMO/HOMO [eV]	Acceptor	V_{OC} [V]	J_{SC} [mA cm^{-2}]	FF [%]	PCE [%]	Ref.
P3b	-3.43/-5.20	N2200	0.78	9.77	60.64	4.67	[43]
DOTFP-PhI	-3.44/-5.44	IT-4F	0.86	17.75	70.1	10.65	[126]
DOTFP-TPD	-3.68/-5.51	IT-4F	0.81	18.34	67.4	10.04	[126]
TPhI-BDT	-3.25/-5.25	IDIC	0.90	14.07	66.0	8.31	[49]
TffPhI-BDT	-3.36/-5.39	IDIC	0.93	15.92	63.9	9.48	[49]
PhI-ffBT	-3.80/-5.55	IT-4F	0.91	19.41	74.2	11.8	[127]
ffPhI-ffBT	-3.86/-5.63	IT-4F	0.94	19.01	71.0	12.74	[127]
PE80	-3.43/-5.50	Y6	0.88	10.24	46.0	4.11	[124]
PE81	-3.46/-5.51	Y6	0.90	19.54	58.0	10.21	[124]
PhI-Th	-2.74/-5.45	Y6	0.80	23.5	55.5	10.5	[128]
PhI-Se	-2.87/-5.61	Y6	0.84	20.7	59.8	10.4	[128]
PhI-Th:PM6	—	Y6	0.84	25.9	71.8	15.6	[128]
PhI-Se:PM6	—	Y6	0.85	25.7	75.5	16.4	[128]
PhI-Th:PM6	—	Y6:PC ₇₁ BM	0.85	26.3	76.8	17.2	[128]
PhI-Se:PM6	—	Y6:PC ₇₁ BM	0.85	24.8	72.1	15.2	[128]
PM6	-3.65/-5.54	Y6	0.84	26.1	74.8	16.4	[129]
PhI-Cl:PM6	—	Y6	0.84	26.8	75.2	17.0	[129]
PhI-Cl:PM6	—	Y6:PC ₇₁ BM	0.85	27.7	77.1	18.1	[129]

Guo and coworkers synthesized a series of PhI-based polymers by varying the side chains.^[43] Incorporating a single alkoxy substituent and optimizing the S...O interactions afforded polymers P3a-P3c with optimized HOMOs and appropriate aggregation properties. The polymer P3b with the longer-but-less-bulky 3,7-dimethyloctyl side-chain showed the highest PCE of 4.7 % by blending with N2200. They synthesized a D-A1-D-A2 type polymer.^[126] The nonhalogenated processed DOTFP-PhI:IT-4F-based OSCs exhibited a PCE of 10.65 %. Introducing fluorine atoms into the PhI unit was also an effective method to improve the performance of non-fullerene OSCs. Guo *et al.*^[49] synthesized two PhI-based D- π -A polymers. Owing to the stronger electron-withdrawing ability of imide group and fluorine atoms, ffPhI-BDT exhibited a deeper HOMO/LUMO levels of -5.39/ -3.36 eV than that (-5.25 eV/-3.25 eV) of TPhI-BDT. Blending with IDIC, the TffPhI-BDT showed a higher PCE of 9.48 % with a larger V_{OC} of 0.93 V, a J_{SC} of 15.92 mA cm⁻², and an FF of 63.9 %, which significantly out-performed the PCE of 8.31 % for TPhI-BDT. Furthermore, they synthesized two D-A1-D-A2 type polymers ffPhI-ffBT and PhI-ffBT.^[127] Pairing with IT-4F, the polymers ffPhI-ffBT and PhI-ffBT realized high PCEs of 12.74 and 13.31 %, respectively. Zhou *et al.*^[124] synthesized two D- π -A copolymers PE80 and PE81, where thiophene and thiophene [3,2-b]-thiophene (TT) were adopted as the π -bridges. The polymer PE81 with TT as a π bridge exhibited much higher PCE of 10.21 % than 4.11 % for PE80.

The ternary and quaternary strategies are effective methods to improve device performance of OSCs.^[131-133] Using PhI-Se and PhI-Th as polymer donor guest, Zhan and co-workers^[128] fabricated more efficient parallel-like ternary and quaternary devices. The PhI-Se could form individual phase and selectively tune the packing ordering of Y6 phase, resulting in enhanced photocurrent and increased electron mobility. As a result, the PhI-Se:PM6:Y6-based ternary devices exhibited a PCE of 16.4 %, and the PhI-Se:PM6:Y6:PC₇₁BM-based quaternary OSCs obtained the highest PCE of 17.2 %. Through the chlorination, they also synthesized ultra-wide bandgap (2.10 eV) polymer PhI-Cl with a deep HOMO (-5.58 eV) energy level.^[129] The PhI-Cl additive enable PM6: Y6 and PM6: Y6: PC₇₁BM based OSCs to exhibit PCEs over 17 % and 18 %, respectively. These works suggest that PhI is promising building block to construct polymer donors.

3.6. Other Imide-Based Polymers

In addition to NTI, TPD, PhI, BTI, TzBI, many other imide-functionalized building blocks were devised for constructing high-performance polymers.

Compared with DPI unit, the naphthodithiophene imide (NDTI) unit has a larger π -conjugated backbone that could enhance intermolecular π -orbital interactions between polymer chains.^[37] It was firstly synthesized in 2012 by Chi and co-workers.^[134] From starting material 4,5-dibromophthalic acid, 4,5-dibromophthalic imide was prepared by treating with SOCl₂ and refluxing with amine in acetic acid. The 4,5-di(thiophen-3-yl) phthalic imide was synthesized by Stille coupling reaction between 4,5-dibromophthalic imide and the tin reagent of thiophene. NDTI was finally obtained by oxidative cyclization reaction of 4,5-di(thiophen-3-yl) phthalic imide with the iron(III) chloride (Scheme 6, Synthetic route 1). He *et al.* optimized the synthetic route of NDTI by using cyclization method under UV irradiation (Scheme 6, Synthetic route 2).^[37] Wu group presented another approach to synthesize NDTI by direct Stille coupling between 4,5-dibromophthalic imide and (3,3'-bis(trimethylstannyl)-5,5'-diyl)bis(trimethyl-silane)-2,2'-bithiophene to form two C_{sp2}-C_{sp2} bonds in simple one step reaction (Scheme 6, Synthetic route 3).^[55]

Scheme 6 Synthetic Route to NDTI.

Isomerism has become an effective method to enhance photovoltaic performance of OSCs by fine tuning the molecular structure. He and co-workers synthesized two polymers based on the NDTI unit, PAB- α and PAB- γ (Figure 12).^[37] The orientation isomerism of thiophene rings could greatly affect the planarity of the two polymers. Due to smaller torsion angle, the polymer PAB- α have superior molecular planarity, resulting in the stronger intermolecular interactions, more red-shifted absorption, better miscibility and nanophase separation morphology. Thus the PAB- α :Y6-based devices achieved a PCE of 15.05 %, while the PAB- γ -based devices exhibited an efficiency of 0.04 %. Wu *et al.*^[55] developed new NDTI-based polymers PNDT1 and PNDT2 by incorporating different side chains at the N-site of the imide. Compared with the polymer

PAB-*a* with branched alkyl chains, PNDT1 and PNDT2 showed higher crystallinity and hole mobility. By pairing with eC9, the PNDT1, and PNDT2-based PSCs showed overall power conversion efficiency of 17.27 % and 18.13 %, respectively. Importantly, the NDTIs have short π - π stacking and abundant short interactions, and their polymers exhibited superior morphological stability (Figure 13). Therefore, the PNDT2-based OSCs exhibited much better device stability than that of PNDT1, PAB-*a*, and benchmark polymers PM6 and D18.

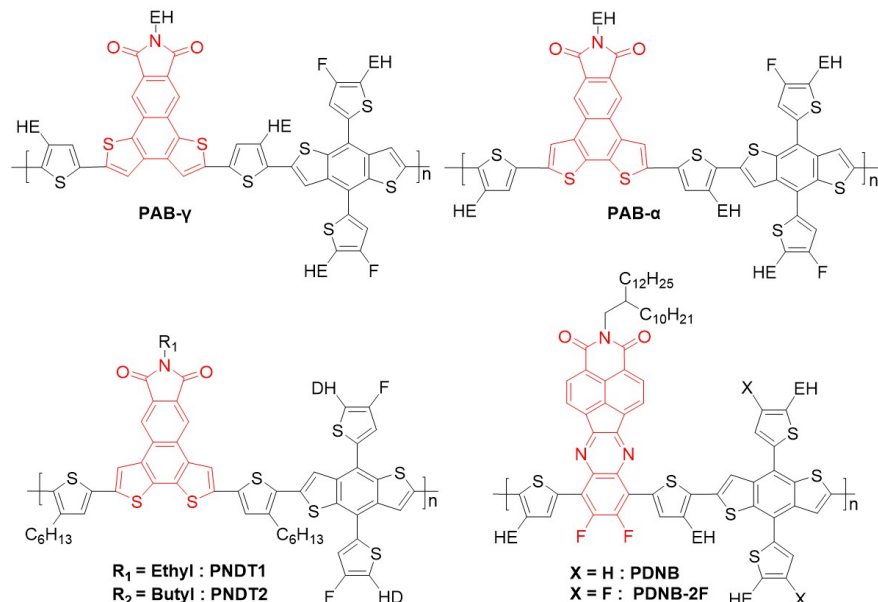


Figure 12 Polymer containing imide-functionalized arenes as electron-acceptor units

Table 7 Summary of the photovoltaic properties of the polymer donors shown in Figure12.

Donor	LUMO/HOMO [eV]	Acceptor	V_{OC} [V]	J_{SC} [mA cm ⁻²]	FF [%]	PCE [%]	Ref.
PAB- <i>a</i>	-3.52/-5.55	Y6	0.90	23.23	72.29	15.05	[37]
PAB- γ	-3.55/-5.43	Y6	0.18	0.74	26.33	0.04	[37]
PNDT1	-3.59/-5.40	eC9	0.87	25.85	0.77	17.27	[55]
PNDT2	-3.58/-5.41	eC9	0.86	26.33	0.80	18.13	[55]
PDNB	-3.91/-5.49	Y6	0.80	16.97	65.47	8.83	[130]
PDNB-2F	-3.95/-5.60	Y6	0.87	22.45	62.37	12.18	[130]

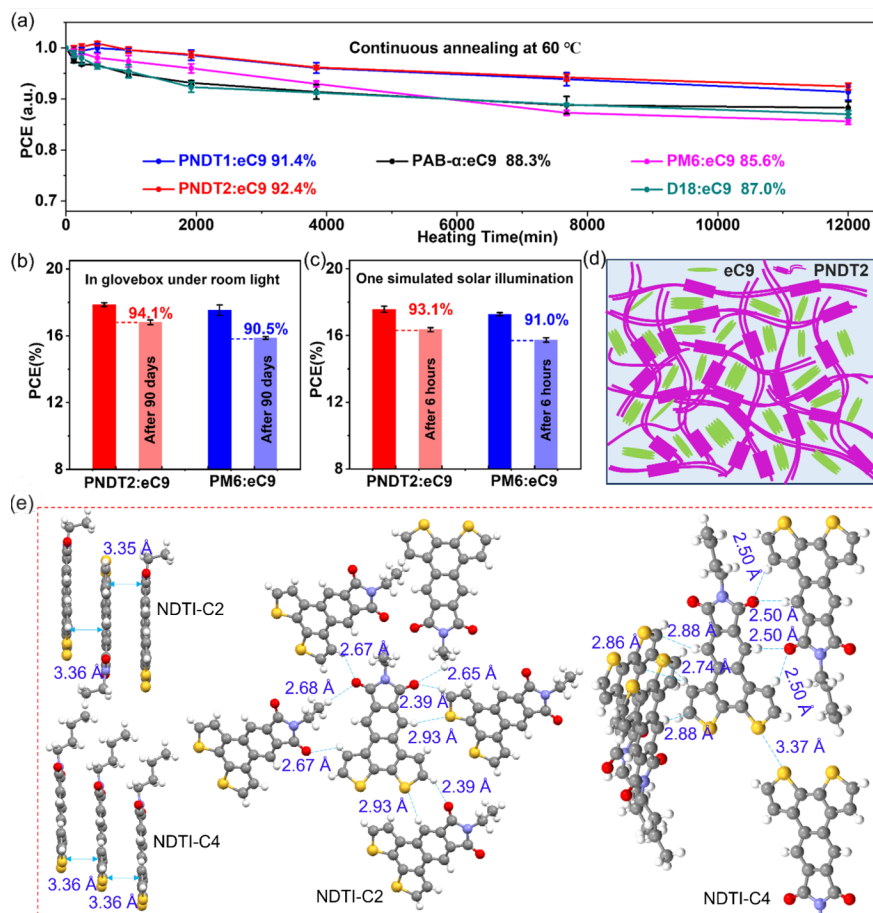


Figure 13 (a) Thermal stability of PNDT12:eC9, PAB- α :eC9, PM6:eC9 and D18:eC9 based OSCs; (b) The shelf stability of PNDT2:eC9 and PM6:eC9 based device in N₂-filled glovebox under room light; (c) The stability of PNDT2:eC9 and PM6:eC9 based device under one simulated solar illumination; (d) Illustration of blend film that compose both polymer and NFA; (e) The single crystal data of NDTI-C2 and NDTI-C4, including the π - π stacking and short interactions between adjacent molecules. Reproduced with permission.^[55] Copyright 2023, American Chemical Society.

Chen *et al.*^[130] used naphthalene imide units as electron withdrawing substituents to develop two difluoro-quinoxaline-based polymer donors, namely PDNB and PDNB-2F (Figure 12). The difluoro-quinoxaline with a naphthalimide substituent not only could downshift copolymer HOMO level, but also the rigid and good planarity backbone could promote intra-molecular charge transfer. Besides, the N-alkyl side chain could guarantee good solubility of copolymers. When blended with an NFA of Y6, the PDNB-2F showed a higher PCE of 12.18 % with a larger V_{OC} of 0.87 V, aJ_{SC} of 22.45 mA cm⁻², and FF of 62.4 %, whereas the device based on PDNB:Y6 showed a comparatively lower PCE of 8.83 % with a V_{OC} of 0.80 V.

Scheme 7 Synthetic Route to DPI/DTID.

Zhan *et al.* firstly reported the synthesis of dithienophthalimide (DPI) from starting material of maleic anhydride in 2011.^[35] Treating maleic anhydride with amine, followed by Suzuki coupling reaction and oxidative cyclization reaction with the iron(III) chloride, DPI could be synthesized efficient (Scheme 7, Synthetic route 1). The dithieno[2,3-e:3',2'-g]isoindole-7,9(8H)-dione (DTID),^[135] an isomer of DPI, could also be synthesized using this approach. Zhao *et al.* reported another synthetic route of DPI from starting material of (3,3'-dibromo-[2,2'-bithiophene]-5,5'-diyl)bis(trimethylsilane). A Cr-mediated cyclization reaction

of (3,3'-dibromo-[2,2'-bithiophene]-5,5'-diyl)bis(trimethylsilane) with dimethyl acetylenedicarboxylate yield benzo[2,1-b:3,4-b']dithiophene-4,5-dicarboxylate. Further alkaline hydrolysis, anhydride and imide formation, DPI was synthesized accordingly (Scheme 7, Synthetic route 2). As a fused-ring building block, the high coplanarity and rigidity, existence of two vacant outer α -positions, and suitable π -electron-deficient ability of DPI make it an ideal electron-deficient building unit for polymer donors. Zhan *et al.* [35] reported the first DPI-based polymer donor P1, which exhibited a PCE of 0.3 % by matching with PC₆₁BM. The chemical structures of some DPI-based conjugated polymers are illustrated in Figure 14 and the photovoltaic properties are summarized in Table 8.

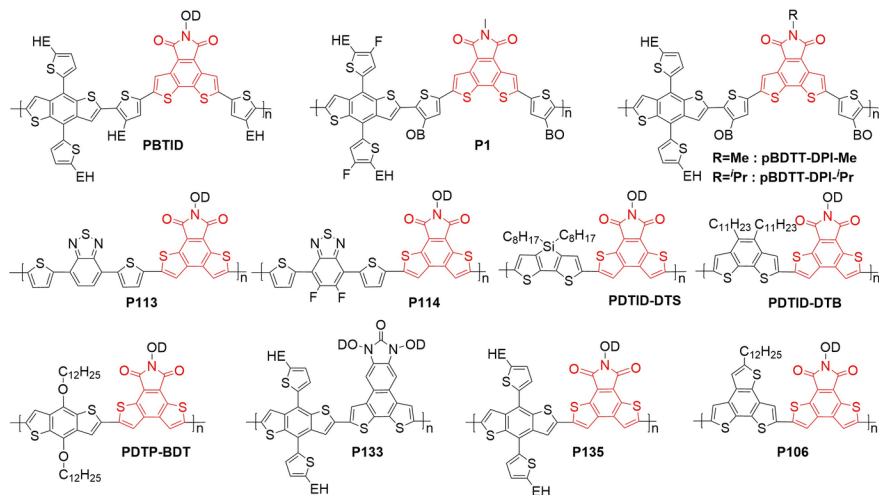


Figure 14 The chemical structures of DPI/DTID-based conjugated polymers.

Table 8 Summary of the photovoltaic properties of the polymer donors shown in Figure 14.

Donor	LUMO/HOMO [eV]	Acceptor	V_{OC} [V]	J_{SC} [mA cm ⁻²]	FF [%]	PCE [%]
P1	-2.78/-5.54	N3	0.90	24.52	65.8	14.52
P1	—	IT-4F	0.95	20.31	64.6	12.46
pBDTT-DPI-Me	-3.60/-5.52	Y6	0.84	26.35	71.15	15.82
pBDTT-DPI-ⁱPr	-3.59/-5.64	Y6	0.87	21.37	59.79	11.08
pBDTT-DPI-Me	—	Y6	0.83	27.42	72.56	16.55
PBTID	-3.54/-5.53	Y6	0.87	26.1	69.6	15.8
P113	-3.64/-5.36	ITIC-m	1.02	12.68	54.0	6.98
P114	-3.77/-5.54	ITIC-m	0.97	16.43	65.4	10.42
PDTID-DTS	-3.51/-5.37	BThIND-Cl	0.92	23.25	0.69	14.76
PDTID-DTB	-3.39/-5.67	BThIND-Cl	1.02	13.36	0.53	7.22
PDTP-BDT	-3.53/-5.46	BThIND-Cl	0.97	21.48	0.63	13.13
P133	-3.54/-5.58	Y6	0.89	18.56	0.62	10.24
P135	-3.32/-5.52	Y6	0.87	24.46	0.71	15.11
P106	-3.52/-5.56	Y18-DMO	0.87	22.78	0.71	14.07
P106	—	Y18-DMO: DBTB-IC	0.91	24.82	0.73	16.49

Ding *et al.* [136] synthesized DPI-based polymer P1 for nonfullerene OSCs. Compared with the thiadiazole in DTBT, the imide is more electron-deficient unit which endows polymer P1 with a deeper HOMO and high V_{OC} (> 0.9 V) value. Moreover, the extended π -conjugation of DPI facilitates polymer packing and charge

transport. The best P1:N3 cells gave a PCE of 14.52 %. Zhao *et al.* [137] synthesized two nonhalogenated DPI-based polymers (pBDTT-DPI-Me and pBDTT-DPI-*i* Pr) by incorporating different side chains at the N-site of the imide to regulate the polymer's solubility and aggregation tendency. The pBDTT-DPI-Me showed stronger aggregation than pBDTT-DPI-*i* Pr in solution. The optimized pBDTT-DPI-Me:Y6-based device showed a PCE of 15.82 %, which is much higher than 11.08 % for pBDTT-DPI-*i* Pr:Y6. Moreover, the efficiency of the pBDTT-DPI-Me:Y6-based Q-PHJ was further improved to 16.55 % owing to the higher charge carrier mobility, more efficient exciton dissociation, and less charge recombination. Zhang *et al.* [52] synthesized polymer PBTID which shows a strong and broad absorption, proper aggregation degree, high hole mobility and a deep-lying HOMO level of -5.53 eV. The PBTID:Y6 devices afforded a PCE of 15.8 %.

Sharma and co-workers reported DTID-based polymers P113 and P114.[135] The absorption coefficient, hole transport mobility, and relative dielectric constant of the polymer P114 with fluorine substitutions are higher than that for P113. A PCE of 10.42 % was obtained for P114:ITIC-m based devices, which is higher than that 8.44 % for P113. They also synthesized three polymers to investigate the effect of different donor unit on the optical and electro-chemical properties.[138] Owing to the different electron-donating abilities of donor units, the HOMO energy levels of PDTID-DTS, PDTID-DTB and PDTP-BDT were estimated as -5.37 eV, -5.67 eV, -5.46 eV, respectively. By blending with BThIND-Cl, the PDTID-DTS, PDTID-DTB and PDTP-BDT-based OSCs showed PCE of 14.76 %, 7.22 % and 13.13 %, respectively. They further compared the photovoltaic performance of polymers P135 and P133 which were developed from DPI and DTNI.[42] The P135 showed higher dielectric constant and dipole moment than P133 owing to the stronger electron-withdrawing of DPI. The PSCs based on P135: Y6 exhibited PCE about 15.11 % which is higher than 10.24 % of P133. The DPI-based polymer P106 with 3TB as the donor unit achieved a PCE of 16.49 % in P106:DBTBT-IC:Y18-DMO based ternary OSCs.[139]

Furthermore, there are some other imide-functionalized electron-deficient building blocks that has not been widely used to construct conjugated polymers for application in non-fullerene based OSCs, such as 2,2'-biazulene-1,1',3,3'-tetracarboxylic diimides (BAzDIs),[140] 1,2,5,6-Naphthalenediimide,[141,142] and dithienyl-benzodiimide (TBDI),[143] which were synthesized for OFETs and all-PSCs.

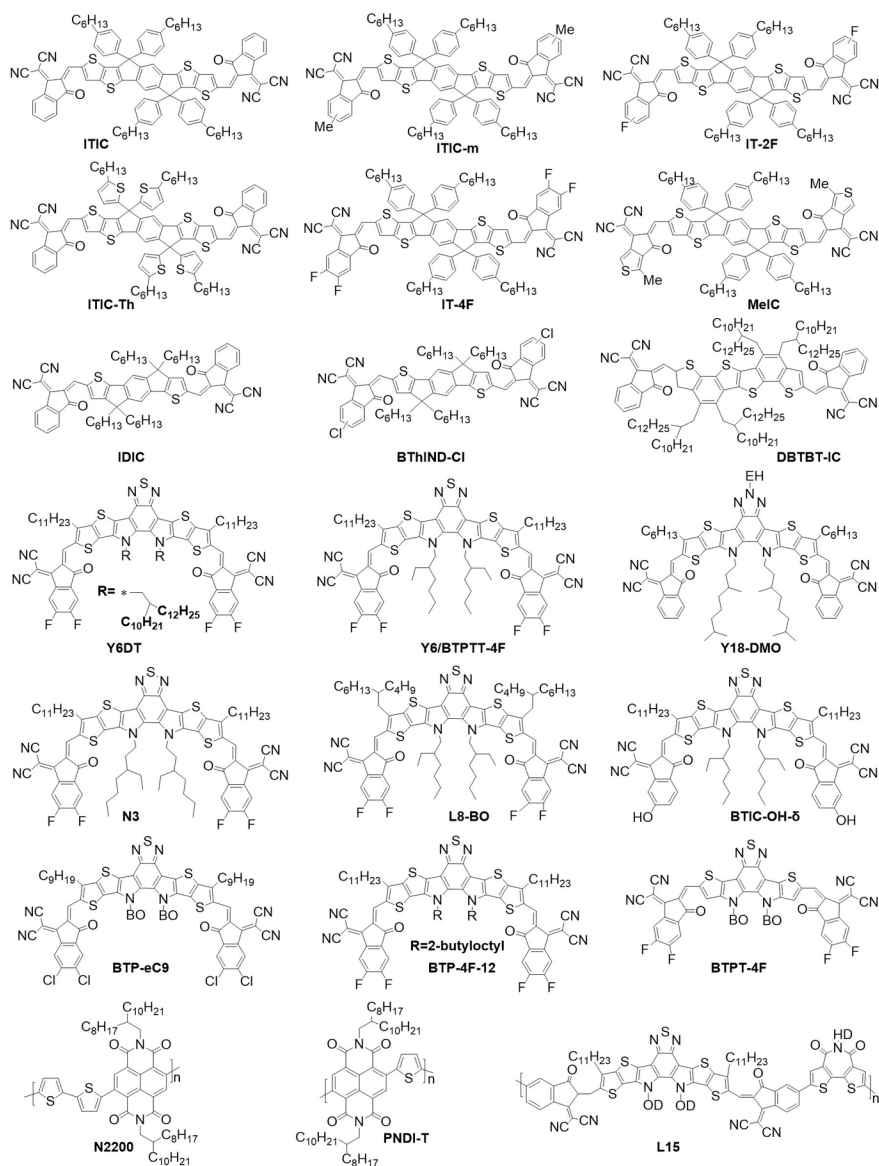


Figure 15 Chemical structures of acceptor materials mentioned.

4. Conclusions and Perspectives

The unique features of imide-functionalized building blocks, including their electron-withdrawing ability, rigid and co-planar structure and easy attachment of various chains on imide functionalities endow them substantial advantages for constructing high-performance organic conjugated polymers. Some of imide-functionalized polymers based OSCs have been realized a PCE as high as 18 %, [33,77,114] which suggest the great promise of imide-functionalized polymer. Despite the numerous imide-functionalized polymers and their enhancing device performances in OSCs, there are still issues that need to be settled down for the future commercialization of imide-functionalized conjugated polymers.

(1) The imide functionalized polymers continue to face the challenge of high cost. There is an urgent need for new synthesis methods and new imide units to simplify the synthesis of high-performance polymers and promote their large-scale production.

(2) How to design new imide functionalized polymers by further reducing energy loss and suppressing charge recombination to further boost efficiency over 20 %.

(3) Further development of high-performance, active layer thickness insensitive and green solvent processing conjugated polymers for organic solar cells.

Acknowledgement

#These authors made equal contribution. This work was supported by the National Natural Science Foundation of China (22179076), Fund for Zhujiang Young Scholar (18220203), Natural Science Foundation of Guangdong Province (2022A1515011803) and the Department of Education of Guangdong Province (2021KCXTD032).

References

1. He, C.; Pan, Y.; Ouyang, Y.; Shen, Q.; Gao, Y.; Yan, K.; Fang, J.; Chen, Y.; Ma, C.-Q.; Min, J.; Zhang, C.; Zuo, L.; Chen, H. Manipulating the D:A interfacial energetics and intermolecular packing for 19.2 % efficiency organic photovoltaics. *Energy Environ. Sci.* **2022**, *15*, 2537-2544.
2. Wei, Y.; Chen, Z.; Lu, G.; Yu, N.; Li, C.; Gao, J.; Gu, X.; Hao, X.; Lu, G.; Tang, Z.; Zhang, J.; Wei, Z.; Zhang, X.; Huang, H. Binary Organic Solar Cells Breaking 19 % via Manipulating the Vertical Component Distribution. *Adv. Mater.* **2022**, *34*, 2204718.
3. Luo, S.; Li, C.; Zhang, J.; Zou, X.; Zhao, H.; Ding, K.; Huang, H.; Song, J.; Yi, J.; Yu, H.; Wong, K. S.; Zhang, G.; Ade, H.; Ma, W.; Hu, H.; Sun, Y.; Yan, H. Auxiliary sequential deposition enables 19 %-efficiency organic solar cells processed from halogen-free solvents. *Nat. Commun.* **2023**, *14*, 6964
4. Lin, Y.; Wang, J.; Zhang, Z. G.; Bai, H.; Li, Y.; Zhu, D.; Zhan, X. An Electron Acceptor Challenging Fullerenes for Efficient Polymer Solar Cells. *Adv. Mater.* **2015**, *27*, 1170-1174.
5. Yuan, J.; Zhang, Y. Q.; Zhou, L. Y.; Zhang, G. C.; Yip, H.-L.; Lau, T.-K.; Lu, X.; Zhu, C.; Peng, H. J.; Johnson, P. A.; Leclerc, M.; Cao, Y.; Ulanski, J.; Li, Y.; Zou, Y. Single-Junction Organic Solar Cell with over 15 % Efficiency Using Fused-Ring Acceptor with Electron-Deficient Core. *Joule* **2019**, *3*, 1140-1151.
6. Li, C.; Zhou, J.; Song, J.; Xu, J.; Zhang, H.; Zhang, X.; Guo, J.; Zhu, L.; Wei, D.; Han, G.; Min, J.; Zhang, Y.; Xie, Z.; Yi, Y.; Yan, H.; Gao, F.; Liu, F.; Sun, Y. Non-fullerene acceptors with branched side chains and improved molecular packing to exceed 18 % efficiency in organic solar cells. *Nat. Energy* **2021**, *6*, 605-613.
7. Jiang, K.; Wei, Q.; Lai, J. Y. L.; Peng, Z.; Kim, H. K.; Yuan, J.; Ye, L.; Ade, H.; Zou, Y.; Yan, H. Alkyl Chain Tuning of Small Molecule Acceptors for Efficient Organic Solar Cells. *Joule* **2019**, *3*, 3020-3033.
8. Li, S.; Li, C.-Z.; Shi, M.; Chen, H. New Phase for Organic Solar Cell Research: Emergence of Y-Series Electron Acceptors and Their Perspectives. *ACS Energy Lett.* **2020**, *5*, 1554-1567.
9. Zhao, W.; Li, S.; Yao, H.; Zhang, S.; Zhang, Y.; Yang, B.; Hou, J. Molecular Optimization Enables over 13 % Efficiency in Organic Solar Cells. *JJ. Am. Chem. Soc.* **2017**, *139*, 7148-7151.
10. Liu, W.; Xu, S.; Lai, H.; Liu, W.; He, F.; Zhu, X. Near-Infrared All-Fused-Ring Nonfullerene Acceptors Achieving an Optimal Efficiency-Cost-Stability Balance in Organic Solar Cells. *CCS Chem.* **2023**, *5*, 654-668.
11. Lai, H. J.; Lai, X.; Chen, Z.-Y.; Zhu, Y.; Wang, H.; Chen, H.; Tan, P.; Zhu, Y.; Zhang, Y.; He, F. Crystallography, Packing Mode, and Aggregation State of Chlorinated Isomers for Efficient Organic Solar Cells. *CCS Chem.* **2022**, *5*, 1118-1129.
12. Tan, P.; Cao, C.; Cheng, Y.; Chen, H.; Lai, H.; Zhu, Y.; Han, L.; Qu, J.; Zheng, N.; Zhang, Y.; He, F. Achieving high performance organic solar cells with a closer π - π distance in branched alkyl-chain acceptors. *J. Mater. Chem. A* **2023**, *11*, 9538-9545.
13. Wang, H. Q.; Han, L.; Zhou, J. D.; Liu, T.; Mo, D. Z.; Chen, H.; Lai, H.; Zheng, N.; Xie, Z. Q.; Zheng, W. H.; He, F. Isomerism: Minor Changes in the Bromine Substituent Positioning Lead to Notable Differences in Photovoltaic Performance. *CCS Chem.* **2021**, *3*, 2591-2601
14. He, K.; Kumar, P.; Yuan, Y.; Li, Y. Wide bandgap polymer donors for high efficiency non-fullerene

- acceptor based organic solar cells. *Mater. Adv.* **2021**, *2*, 115-145.
15. Ning, H. J.; Zhang, G. Y.; Chen, H.; Wang, Z.; Ni, S.; Lu, F.; Liu, F.; Dang, L.; Liu, J.; He, F.; Wu, Q. H. Naphthalenothiophene Imide-Based Polymer Donor for High-Performance Polymer Solar Cells. *Chem. Mater.* **2021**, *33*, 1976-1982.
 16. Ning, H.; Jiang, Q.; Han, P.; Lin, M.; Zhang, G.; Chen, J.; Chen, H.; Zeng, S.; Gao, J.; Liu, J.; He, F.; Wu, Q. Manipulating the solubility properties of polymer donors for high-performance layer-by-layer processed organic solar cells. *Energy Environ. Sci.* **2021**, *14*, 5919-5928.
 17. Fu, H.; Wang, Z.; Sun, Y. Polymer Donors for High-Performance Non-Fullerene Organic Solar Cells. *Angew. Chem., Int. Ed.* **2019**, *58*, 4442-4453.
 18. Han, P. W.; Lin, M.; Jiang, Q.J.; Ning, H.J.; Su, M.B.; Dang, L.; He, F.; Wu, Q. H. Ladder-Type Thienoacenaphthopyrazine-Based Molecules: Synthesis, Properties, and Application to Construct High-Performance Polymer for Organic Solar Cells. *CCS Chem.* **2023**, *5*, 1318-1331.
 19. Zhao, T.; Cao, C.; Wang, H.; Shen, X.; Lai, H.; Zhu, Y.; Chen, H.; Han, L.; Rehman, T.; He, F. Highly Efficient All-Polymer Solar Cells from a Dithieno[3,2-f:2',3'-h]quinoxaline-Based Wide Band Gap Donor. *Macromolecules* **2021**, *54*, 11468-11477.
 20. Xiao, M.; Liu, L.; Meng, Y.; Fan, B.; Su, W.; Jin, C.; Liao, L.; Yi, F.; Xu, C.; Zhang, R.; Jen, A. K. Y.; Ma, W.; Fan, Q. Approaching 19 % efficiency and stable binary polymer solar cells enabled by a solidification strategy of solvent additive. *Sci. China Chem.* **2023**, *66*, 1500-1510.
 21. Cui, Y.; Xu, Y.; Yao, H.; Bi, P.; Hong, L.; Zhang, J.; Zu, Y.; Zhang, T.; Qin, J.; Ren, J.; Chen, Z.; He, C.; Hao, X.; Wei, Z.; Hou, J. Single-Junction Organic Photovoltaic Cell with 19 % Efficiency. *Adv. Mater.* **2021**, *33*, 2102420.
 22. Zhang, G.Y.; Ning, H. J.; Chen, H.; Jiang, Q. J.; Jiang, J. Q.; Han, P. W.; Dang, L.; Xu, M.; Shao, M.; He, F.; Wu, Q. H. Naphthalenothiophene imide-based polymer exhibiting over 17 % efficiency. *Joule* **2021**, *5*, 931-944.
 23. Samson, S.; Rech, J.; Perdígón-Toro, L.; Peng, Z.; Shoaee, S.; Ade, H.; Neher, D.; Stolterfoht, M.; You, W. Organic Solar Cells with Large Insensitivity to Donor Polymer Molar Mass across All Acceptor Classes. *ACS Appl. Polym. Mater.* **2020**, *2*, 5300-5308.
 24. Li, D. Y.; Wang, H. J.; Chen, J. M.; Wu, Q. H. Fluorinated Polymer Donors for Nonfullerene Organic Solar Cells. *Chem. Eur. J.* **2023**, *n/a*, e202303155
 25. Pron, A.; Leclerc, M. Imide/amide based π -conjugated polymers for Organic Electronics. *Prog. Polym. Sci.* **2013**, *38*, 1815-1831.
 26. Sun, H. L.; Wang, L.; Wang, Y.; Guo, X. Imide-Functionalized Polymer Semiconductors. *Chem. Eur. J.* **2018**, *25*, 87-105.
 27. Nielsen, C. B.; Ashraf, R. S.; Treat, N. D.; Schroeder, B. C.; Donaghey, J. E.; White, A. J. P.; Stingelin, N.; McCulloch, I. 2,1,3-Benzothiadiazole-5,6-Dicarboxylic Imide – A Versatile Building Block for Additive- and Annealing-Free Processing of Organic Solar Cells with Efficiencies Exceeding 8 %. *Adv. Mater.* **2015**, *27*, 948-953.
 28. Guo, X. G.; Ortiz, R. P.; Zheng, Y.; Hu, Y.; Noh, Y.-Y.; Baeg, K.-J.; Facchetti, A.; Marks, T. J. Bithiophene-Imide-Based Polymeric Semiconductors for Field-Effect Transistors: Synthesis, Structure-Property Correlations, Charge Carrier Polarity, and Device Stability. *J. Am. Chem. Soc.* **2011**, *133*, 1405-1418.
 29. Qiao, X. L.; Chen, W. C.; Wu, Q. H.; Zhang, S. Q.; Wu, H. Z.; Liu, Z.; Yang, R. Q.; Li, H. X. Bithienopyrroledione vs. thienopyrroledione based copolymers: dramatic increase of power conversion efficiency in bulk heterojunction solar cells. *Chem. Commun.* **2017**, *53*, 3543-3546.
 30. Liao, M.; Duan, J.; Peng, P. a.; Zhang, J.; Zhou, M. Progress in the synthesis of imide-based N-type polymer semiconductor materials. *RSC Adv.* **2020**, *10*, 41764-41779.
 31. Ha, J.-W.; Park, H. J.; Kang, I.-N.; Hwang, D.-H. Bithienopyrroledione-based polymeric donors for efficient fullerene- and non-fullerene-based organic photovoltaic cells. *Dyes Pigments* **2022**, *200*, 110176.
 32. Guo, X.; Zhou, N.; Lou, S. J.; Hennek, J. W.; Ponce Ortiz, R.; Butler, M. R.; Boudreault, P.-L. T.; Strzalka, J.; Morin, P.-O.; Leclerc, M.; López Navarrete, J. T.; Ratner, M. A.; Chen, L. X.; Chang,

- R. P. H.; Facchetti, A.; Marks, T. J. Bithiopheneimide–Dithienosilole/Dithienogermole Copolymers for Efficient Solar Cells: Information from Structure–Property–Device Performance Correlations and Comparison to Thieno[3,4-c]pyrrole-4,6-dione Analogues. *J. Am. Chem. Soc.* **2012**, *134*, 18427-18439.
33. Jiang, Q. J.; Han, P. W.; Ning, H. J.; Jiang, J. Q.; Chen, H.; Xiao, Y.; Ye, C.-R.; Chen, J.; Lin, M.; He, F.; Huang, X.-C.; Wu, Q. H. Reducing steric hindrance around electronegative atom in polymer simultaneously enhanced efficiency and stability of organic solar cells. *Nano Energy* **2022**, *101*, 107611.
 34. Guo, X. G.; Facchetti, A.; Marks, T. J. Imide- and Amide-Functionalized Polymer Semiconductors. *Chem. Rev.* **2014**, *114*, 8943-9021.
 35. Wang, H.; Shi, Q.; Lin, Y.; Fan, H.; Cheng, P.; Zhan, X.; Li, Y.; Zhu, D. Conjugated Polymers Based on a New Building Block: Dithienophthalimide. *Macromolecules* **2011**, *44*, 4213-4221.
 36. Letizia, J. A.; Salata, M. R.; Tribout, C. M.; Facchetti, A.; Ratner, M. A.; Marks, T. J. n-Channel Polymers by Design: Optimizing the Interplay of Solubilizing Substituents, Crystal Packing, and Field-Effect Transistor Characteristics in Polymeric Bithiophene-Imide Semiconductors. *J. Am. Chem. Soc.* **2008**, *130*, 9679-9694.
 37. Shen, X.; Lai, X.; Lai, H.; Zhao, T.; Zhu, Y.; Pu, M.; Wang, H.; Tan, P.; He, F. Isomerism Strategy to Optimize Aggregation and Morphology for Superior Polymer Solar Cells. *Macromolecules* **2022**, *55*, 6384-6393.
 38. Hadmojo, W. T.; Wibowo, F. T. A.; Ryu, D. Y.; Jung, I. H.; Jang, S.-Y. Fullerene-Free Organic Solar Cells with an Efficiency of 10.2 % and an Energy Loss of 0.59 eV Based on a Thieno[3,4-c]Pyrrole-4,6-dione-Containing Wide Band Gap Polymer Donor. *ACS Appl. Mater. Interfaces* **2017**, *9*, 32939-32945.
 39. Yasa, M.; Toppare, L. Thieno[3,4-c]pyrrole-4,6-dione-Based Conjugated Polymers for Nonfullerene Organic Solar Cells. *Macromol. Chem. Phys.* **2022**, *223*.
 40. Zhou, Y.; Zhang, W.; Yu, G. Recent structural evolution of lactam- and imide-functionalized polymers applied in organic field-effect transistors and organic solar cells. *Chem. Sci.* **2021**, *12*, 6844-6878.
 41. Dutta, T., Li, Y., Thornton, A.L., Zhu, D.-M. and Peng, Z. Imide-functionalized naphthodithiophene based donor-acceptor conjugated polymers for solar cells. *J. Polym. Sci. Part A: Polym. Chem.* **2013**, *51*, 3818-3828
 42. Keshtov, M.L., Shikin, D.Y., Khokhlov, A.R., Ostapov, I.E., Alekseev, V.G., Singh, M.K. and Sharma, G.D. Dithieno[2,3-e:3',2'-g]isoindole-7,9(8H)-Dione and Dithieno[3',2':5,6;2'',3'':7,8]naphtho[2,3-d]imidazol-9(10H)-One-Based Wide Bandgap Copolymer for Efficient Polymer Solar Cells. *Energy Technol.* **2023**, *11*, 2201211.
 43. Chen, J. H.; Qiu, F. L.; Liao, Q. G.; Peng, C. L.; Liu, F.; Guo, X. G. Side-Chain Optimization of Phthalimide-Bithiophene Copolymers for Efficient All-Polymer Solar Cells with Large Fill Factors. *Asian J. Org. Chem.* **2018**, *7*, 2239-2247.
 44. Guo, X. G.; Kim, F. S.; Seger, M. J.; Jenekhe, S. A.; Watson, M. D. Naphthalene Diimide-Based Polymer Semiconductors: Synthesis, Structure–Property Correlations, and n-Channel and Ambipolar Field-Effect Transistors. *Chem. Mater.* **2012**, *24*, 1434-1442.
 45. Wu, Q. H.; Zhao, D.; Schneider, A. M.; Chen, W.; Yu, L. Covalently Bound Clusters of Alpha-Substituted PDI—Rival Electron Acceptors to Fullerene for Organic Solar Cells. *J. Am. Chem. Soc.* **2016**, *138*, 7248-7251.
 46. Zhao, C.; Yang, F.; Xia, D.; Zhang, Z.; Zhang, Y.; Yan, N.; You, S.; Li, W. Thieno[3,4-c]pyrrole-4,6-dione-based conjugated polymers for organic solar cells. *Chem. Commun.* **2020**, *56*, 10394-10408.
 47. Lin, F.; Huang, W.; Sun, H.; Xin, J.; Zeng, H.; Yang, T.; Li, M.; Zhang, X.; Ma, W.; Liang, Y. Thieno[3,4-c]pyrrole-4,6(5H)-dione Polymers with Optimized Energy Level Alignments for Fused-Ring Electron Acceptor Based Polymer Solar Cells. *Chem. Mater.* **2017**, *29*, 5636-5645.
 48. Guo, X.; Kim, F. S.; Jenekhe, S. A.; Watson, M. D. Phthalimide-Based Polymers for High Performance Organic Thin-Film Transistors. *J. Am. Chem. Soc.* **2009**, *131*, 7206-7207.
 49. Yu, J.; Yang, J.; Zhou, X.; Yu, S.; Tang, Y.; Wang, H.; Chen, J.; Zhang, S.; Guo, X. Phthalimide-Based Wide Bandgap Donor Polymers for Efficient Non-Fullerene Solar Cells. *Macromolecules* **2017**, *50*, 8928-8937.
 50. Lan, L.; Cai, P.; Mai, Y.; Hu, Z.; Wen, W.; Zhang, J.; Li, Y.; Shi, H.; Zhang, J. A new wide-bandgap

- conjugated polymer based on imide-fused benzotriazole for highly efficient nonfullerene polymer solar cells. *Dyes Pigments* **2018**, *158* , 219-224.
51. Lan, L. Y.; Chen, Z. M.; Hu, Q.; Ying, L.; Zhu, R.; Liu, F.; Russell, T. P.; Huang, F.; Cao, Y. High-Performance Polymer Solar Cells Based on a Wide-Bandgap Polymer Containing Pyrrolo[3,4-f]benzotriazole-5,7-dione with a Power Conversion Efficiency of 8.63 %. *Adv. Sci.* **2016**, *3*, 1600032.
 52. Zhang, L.; Zhang, Z. L.; Liang, H. Y.; Guo, X.; Zhang, M. J. A Non-Halogenated Polymer Donor Based on Imide Unit for Organic Solar Cells with Efficiency Nearly 16 %. *Chin. J. Chem.* **2023**, *41* , 2095-2102.
 53. Feng, K.; Guo, H.; Sun, H.; Guo, X. G. n-Type Organic and Polymeric Semiconductors Based on Bithiophene Imide Derivatives. *Acc. Chem. Res.* **2021**, *54* , 3804-3817.
 54. Li, Z.; Yang, D. L.; Zhao, X. L.; Zhang, T.; Zhang, J.; Yang, X. Achieving an Efficiency Exceeding 10 % for Fullerene-based Polymer Solar Cells Employing a Thick Active Layer via Tuning Molecular Weight. *Adv. Funct. Mater.* **2017**, *28*, 1705257.
 55. Su, M. B.; Lin, M.; Mo, S. M.; Chen, J. M.; Shen, X.; Xiao, Y.; Wang, M.; Gao, J.; Dang, L.; Huang, X.-c.; He, F.; Wu, Q. H. Manipulating the Alkyl Chains of Naphthodithiophene Imide-Based Polymers to Concurrently Boost the Efficiency and Stability of Organic Solar Cells. *ACS Appl. Mater. Interfaces* **2023**, *15* , 37371-37380.
 56. Li, H., Sun, S., Salim, T., Bomma, S., Grimsdale, A.C. and Lam, Y.M. Conjugated polymers based on dicarboxylic imide-substituted isothianaphthene and their applications in solar cells. *J. Polym. Sci. A Polym* **2012**, *50*, 250-260.
 57. Xu, X.; Wang, C.; Backe, O.; James, D. I.; Bini, K.; Olsson, E.; Andersson, M. R.; Fahlman, M.; Wang, E. Pyrrolo[3,4-g]quinoxaline-6,8-dione-based conjugated copolymers for bulk heterojunction solar cells with high photovoltages. *Polym. Chem.* **2015**, *6* , 4624-4633.
 58. Lan, L.; Chen, Z.; Li, Y.; Ying, L.; Huang, F.; Cao, Y. Donor-acceptor conjugated polymers based on cyclic imide substituted quinoxaline or dibenzo[a,c]phenazine for polymer solar cells. *Polym. Chem.* **2015**, *6* , 7558-7569.
 59. Yu, J.; Ornelas, J. L.; Tang, Y.; Uddin, M. A.; Guo, H.; Yu, S.; Wang, Y.; Woo, H. Y.; Zhang, S.; Xing, G.; Guo, X.; Huang, W. 2,1,3-Benzothiadiazole-5,6-dicarboxylicimide-Based Polymer Semiconductors for Organic Thin-Film Transistors and Polymer Solar Cells. *ACS Appl. Mater. Interfaces* **2017**, *9* , 42167-42178.
 60. Wang, L.; Cai, D.; Zheng, Q.; Tang, C.; Chen, S.-C.; Yin, Z. Low Band Gap Polymers Incorporating a Dicarboxylic Imide-Derived Acceptor Moiety for Efficient Polymer Solar Cells. *ACS Macro Letters* **2013**, *2* , 605-608.
 61. Luo, C.; Shen, Z.; Meng, X.; Han, L.; Sun, S.; Lin, T.; Sun, J.; Peng, H.; Chu, J. Design and synthesis of pyromellitic diimide-based donor-acceptor conjugated polymers for photovoltaic application. *Polym. Adv. Technol.* **2014**, *25* , 809-815.
 62. Li, H.; Kim, F. S.; Ren, G.; Hollenbeck, E. C.; Subramaniyan, S.; Jenekhe, S. A. Tetraazabenzodifluoranthene Diimides: Building Blocks for Solution-Processable n-Type Organic Semiconductors. *Angew. Chem. Int. Ed.* **2013**, *52* , 5513-5517.
 63. Yan, C.; Barlow, S.; Wang, Z.; Yan, H.; Jen, A. K. Y.; Marder, S. R.; Zhan, X. Non-fullerene acceptors for organic solar cells. *Nat. Rev. Mater.* **2018**, *3* , 18003.
 64. Zhang, G.; Zhao, J.; Chow, P. C. Y.; Jiang, K.; Zhang, J.; Zhu, Z.; Zhang, J.; Huang, F.; Yan, H. Nonfullerene Acceptor Molecules for Bulk Heterojunction Organic Solar Cells. *Chem. Rev.* **2018**, *118* , 3447-3507.
 65. Zhou, N.; Facchetti, A. Naphthalenediimide (NDI) polymers for all-polymer photovoltaics. *Mater. Today* **2018**, *21* , 377-390.
 66. Hwang, H.; Ko, H.; Park, S.; Suranagi, S. R.; Sin, D. H.; Cho, K. Fluorine-functionalization of an isoindoline-1,3-dione-based conjugated polymer for organic solar cells. *Org. Electron.* **2018**, *59* , 247-252.
 67. Xu, W.; Li, X.; Jeong, S. Y.; Son, J. H.; Zhou, Z.; Jiang, Q.; Woo, H. Y.; Wu, Q.; Zhu, X.; Ma, X.; Zhang, F. Achieving 17.5 % efficiency for polymer solar cells via a donor and acceptor layered

- optimization strategy. *J. Mater. Chem. C* **2022**, *10* , 5489-5496.
68. Ma, X.; Jiang, Q.; Xu, W.; Xu, C.; Young Jeong, S.; Young Woo, H.; Wu, Q.; Zhang, X.; Yuan, G.; Zhang, F. Layered optimization strategy enables over 17.8 % efficiency of layer-by-layer organic photovoltaics. *Chem. Eng. J.* **2022**, *442* , 136368.
 69. Li, Y.; Chen, H.; Lai, H. J.; Lai, X.; Rehman, T.; Zhu, Y.; Wang, Y.; Wu, Q.; He, F. Efficient and Stable Quasiplanar Heterojunction Solar Cells with an Acetoxy-Substituted Wide-Bandgap Polymer. *ACS Mater. Lett.* **2022**, *4* , 1322-1331.
 70. Chen, H.; Lai, H. J.; Jiang, Q. J.; Lai, X.; Zhu, Y.; Qu, J.; Wu, Q.; He, F. 3D network acceptor with gradient hydrogen bond interaction as a bifunctional layer in quasiplanar heterojunction organic solar cells. *Nano Energy* **2023**, *113* ,108593.
 71. Gao, Y.; Liao, J.; Chen, H.; Ning, H.; Wu, Q. H.; Li, Z.; Wang, Z.; Zhang, X.; Shao, M.; Yu, Y. High Performance Polarization-Resolved Photodetectors Based on Intrinsically Stretchable Organic Semiconductors. *Adv. Sci.* **2022**, *10* .
 72. Sice, J. SUBSTITUTED THENOIC ACIDS. *J. Org. Chem.***1954**, *19* , 70-73.
 73. Zhang, Q. T.; Tour, J. M. Low Optical Bandgap Polythiophenes by an Alternating Donor/Acceptor Repeat Unit Strategy. *J. Am. Chem. Soc.* **1997**, *119* , 5065-5066.
 74. Nielsen, C. B.; Bjornholm, T. New Regiosymmetrical Dioxopyrrolo- and Dihydropyrrolo-Functionalized Polythiophenes. *Org. Lett.***2004**, *6* , 3381-3384.
 75. Berrouard, P.; Grenier, F.; Pouliot, J.-R.; Gagnon, E.; Tessier, C.; Leclerc, M. Synthesis and Characterization of 5-Octylthieno[3,4-c]pyrrole-4,6-dione Derivatives As New Monomers for Conjugated Copolymers. *Org. Lett.* **2011**, *13* , 38-41.
 76. Fuse, S.; Takahashi, R.; Takahashi, T. Facile, One-Step Synthesis of 5-Substituted Thieno[3,4-c]pyrrole-4,6-dione by Palladium-Catalyzed Carbonylative Amidation. *Eur. J. Org. Chem.***2015**, *2015* , 3430-3434.
 77. Xu, L.-Y.; Gao, Y.; Wang, W.; Shao, Y.; Chen, M.; Yang, X.; Fu, Y.; Zhang, M.; Lu, X.; Sun, R.; Min, J. A facile synthetic approach based on thieno[3,4-c]pyrrole-4,6-dione to construct polymer donors for highly efficient organic solar cells. *Energy Environ. Sci.***2023**, *16* , 3942-3950.
 78. Xu, X. F.; Li, Z. J.; Zhang, W.; Meng, X.; Zou, X. S.; Di Carlo Rasi, D.; Ma, W.; Yartsev, A.; Andersson, M. R.; Janssen, R. A. J.; Wang, E. 8.0 % Efficient All-Polymer Solar Cells with High Photovoltage of 1.1 V and Internal Quantum Efficiency near Unity. *Adv. Energy Mater.* **2017**, *8* ,1700908.
 79. Zhao, B. F.; Wu, H. M.; Wang, W. P.; Liu, H. L.; Liu, J.; Cong, Z. Y.; Gao, C. Efficient non-fullerene polymer solar cells enabled by side-chain conjugated thieno[3,4-c]pyrrole-4,6-dione-based polymer and small molecular acceptors. *React. Funct. Polym.***2019**, *145* , 104378.
 80. Liao, C.-Y.; Chen, Y.; Lee, C.-C.; Wang, G.; Teng, N.-W.; Lee, C.-H.; Li, W.-L.; Chen, Y.-K.; Li, C.-H.; Ho, H.-L.; Tan, P. H.-S.; Wang, B.; Huang, Y.-C.; Young, R. M.; Wasielewski, M. R.; Marks, T. J.; Chang, Y.-M.; Facchetti, A. Processing Strategies for an Organic Photovoltaic Module with over 10 % Efficiency. *Joule* **2020**,*4* , 189-206.
 81. Wu, J.; Liao, C.-Y.; Chen, Y.; Jacobberger, R. M.; Huang, W.; Zheng, D.; Tsai, K.-W.; Li, W.-L.; Lu, Z.; Huang, Y.; Wasielewski, M. R.; Chang, Y.-M.; Marks, T. J.; Facchetti, A. To Fluorinate or Not to Fluorinate in Organic Solar Cells: Achieving a Higher PCE of 15.2 % when the Donor Polymer is Halogen-Free. *Adv. Energy Mater.***2021**, *11* , 2102648.
 82. Park, J. S.; Kim, G. U.; Lee, D.; Lee, S.; Ma, B.; Cho, S.; Kim, B. J. Importance of Optimal Crystallinity and Hole Mobility of BDT-Based Polymer Donor for Simultaneous Enhancements of Voc, Jsc, and FF in Efficient Nonfullerene Organic Solar Cells. *Adv. Funct. Mater.***2020**, *30* , 2005787.
 83. Park, J. B.; Ha, J.-W.; Jung, I. H.; Hwang, D.-H. High-Performance Nonfullerene Organic Photovoltaic Cells Using a TPD-Based Wide Bandgap Donor Polymer. *ACS Appl. Energy Mater.* **2019**, *2* , 5692-5697.
 84. Zhang, C.-H.; Wang, W.; Huang, W.; Wang, J.; Hu, Z.; Lin, Z.; Yang, T.; Lin, F.; Xing, Y.; Bai, J.; Sun, H.; Liang, Y. Methyl Thioether Functionalization of a Polymeric Donor for Efficient Solar Cells Processed from Non-Halogenated Solvents. *Chem. Mater.***2019**, *31* , 3025-3033.

85. Yang, N.; Cheng, Y.; Kim, S.; Huang, B.; Liu, Z.; Deng, J.; Wang, J.; Yang, C.; Wu, F.; Chen, L. Random Copolymerization Strategy for Host Polymer Donor PM6 Enables Improved Efficiency Both in Binary and Ternary Organic Solar Cells. *ChemSusChem* **2022**, *15*, e202200138.
86. Pang, S. T.; Zhang, R. W.; Duan, C. H.; Zhang, S.; Gu, X. D.; Liu, X.; Huang, F.; Cao, Y. Alkyl Chain Length Effects of Polymer Donors on the Morphology and Device Performance of Polymer Solar Cells with Different Acceptors. *Adv. Energy Mater.* **2019**, *9*, 1901740.
87. Yasa, M.; Depci, T.; Alemdar, E.; Hacioglu, S. O.; Cirpan, A.; Toppare, L. Non-fullerene organic photovoltaics based on thienopyrroledione comprising random copolymers; effect of alkyl chains. *Renew. Energy* **2021**, *178*, 202-211.
88. Zou, Y.; Najari, A.; Berrouard, P.; Beaupre, S.; Reda Aich, B.; Tao, Y.; Leclerc, M. A Thieno[3,4-c]pyrrole-4,6-dione-Based Copolymer for Efficient Solar Cells. *J. Am. Chem. Soc.* **2010**, *132*, 5330-5331.
89. Chen, J.; Cao, Y. Development of Novel Conjugated Donor Polymers for High-Efficiency Bulk-Heterojunction Photovoltaic Devices. *Acc. Chem. Res.* **2009**, *42*, 1709-1718.
90. Li, Y. Molecular Design of Photovoltaic Materials for Polymer Solar Cells: Toward Suitable Electronic Energy Levels and Broad Absorption. *Acc. Chem. Res.* **2012**, *45*, 723-733.
91. Fan, Q.; Fu, H.; Wu, Q.; Wu, Z.; Lin, F.; Zhu, Z.; Min, J.; Woo, H. Y.; Jen, A. K. Y. Multi-Selenophene-Containing Narrow Bandgap Polymer Acceptors for All-Polymer Solar Cells with over 15 % Efficiency and High Reproducibility. *Angew. Chem. Int. Ed.* **2021**, *60*, 15935-15943.
92. Britel, O.; Fitri, A.; Benjelloun, A. T.; Slimi, A.; Benzakour, M.; McHarfi, M. Theoretical investigation of the influence of π -spacer on photovoltaic performances in carbazole-based dyes for dye-sensitized solar cells applications. *J. Photochem. Photobiol. A Chem.* **2022**, *428*, 113870.
93. Agneeswari, R.; Kim, D.; Park, S. W.; Jang, S.; Yang, H. S.; Shin, I.; Jeong, J. H.; Tamilaivan, V.; Jung, Y. K.; Park, S. H. Influence of thiophene and furan π -bridge on the properties of poly(benzodithiophene-alt-bis(π -bridge)pyrrolopyrrole-1,3-dione) for organic solar cell applications. *Polymer* **2021**, *229*, 123991.
94. Yilmaz, E. A.; Yasa, M.; Cirpan, A.; Toppare, L. A follow-up investigation: Organic solar cells based on chalcogenophene-Thieno[3,4-c]pyrrole-4,6-dione-chalcogenophene containing rJ. *Electroanal. Chem.* **2023**, *932*, 117213.
95. Chao, P.; Guo, M.; Zhu, Y.; Chen, H.; Pu, M.; Huang, H.-H.; Meng, H.; Yang, C.; He, F. Enhanced Photovoltaic Performance by Synergistic Effect of Chlorination and Selenophene π -Bridge. *Macromolecules* **2020**, *53*, 2893-2901.
96. Jo, J. W.; Jung, J. W.; Ahn, H.; Ko, M. J.; Jen, A. K. Y.; Son, H. J. Effect of Molecular Orientation of Donor Polymers on Charge Generation and Photovoltaic Properties in Bulk Heterojunction All-Polymer Solar Cells. *Adv. Energy Mater.* **2017**, *7*, 1601365.
97. Li, H.; Liu, F.; Wang, X.; Gu, C.; Wang, P.; Fu, H. Diketopyrrolopyrrole-Thiophene-Benzothiadiazole Random Copolymers: An Effective Strategy To Adjust Thin-Film Crystallinity for Transistor and Photovoltaic Properties. *Macromolecules* **2013**, *46*, 9211-9219.
98. Zhao, J. J.; Li, Q. D.; Liu, S. J.; Cao, Z. X.; Jiao, X. C.; Cai, Y.-P.; Huang, F. Bithieno[3,4-c]pyrrole-4,6-dione-Mediated Crystallinity in Large-Bandgap Polymer Donors Directs Charge Transportation and Recombination in Efficient Nonfullerene Polymer Solar Cells. *ACS Energy Lett.* **2020**, *5*, 367-375.
99. Zhao, J. J.; Huang, X. L.; Li, Q. D.; Liu, S.; Fan, Z.; Zhang, D.; Ma, S.; Cao, Z.; Jiao, X.; Cai, Y.-P.; Huang, F. Shorter alkyl chain in thieno[3,4-c]pyrrole-4,6-dione (TPD)-based large bandgap polymer donors – Yield efficient non-fullerene polymer solar cells. *J. Energy Chem.* **2021**, *53*, 69-76.
100. Li, Q.; Huang, X.; Liu, S.; Zhao, J.; Zou, Y.; Ding, Y.; Cao, Z.; Jiao, X.; Cai, Y.-P. The alkyl chain positioning of thieno[3,4-c]pyrrole-4,6-dione (TPD)-Based polymer donors mediates the energy loss, charge transport and recombination in polymer solar cells. *J. Power Sources* **2020**, *480*, 229098.
101. Berrouard, P.; Grenier, F.; Pouliot, J.-R.; Gagnon, E.; Tessier, C.; Leclerc, M. Synthesis and Characterization of 5-Octylthieno[3,4-c]pyrrole-4,6-dione Derivatives As New Monomers for Conjugated Copolymers. *Org. Lett.* **2011**, *13*, 38-41.
102. Qiao, X.; Wu, Q.; Wu, H.; Wang, D.; Li, H. High performance thin film transistors based on bi-

- thieno[3,4-c]pyrrole-4,6-dione-containing copolymers: tuning the face-on and edge-on packing orientations. *Polym. Chem.***2016**, *7* , 807-815.
103. Fan, B. B.; Ying, L.; Wang, Z. F.; He, B.; Jiang, X.-F.; Huang, F.; Cao, Y. Optimisation of processing solvent and molecular weight for the production of green-solvent-processed all-polymer solar cells with a power conversion efficiency over 9 %. *Energy Environ. Sci.***2017**, *10* , 1243-1251.
 104. Fan, B. B.; Zhang, K.; Jiang, X. F.; Ying, L.; Huang, F.; Cao, Y. High-Performance Nonfullerene Polymer Solar Cells based on Imide-Functionalized Wide-Bandgap Polymers. *Adv. Mater.***2017**, *29* .
 105. Zhong, W.; Li, K.; Cui, J.; Gu, T.; Ying, L.; Huang, F.; Cao, Y. Efficient All-Polymer Solar Cells Based on Conjugated Polymer Containing an Alkoxyated Imide-Functionalized Benzotriazole Unit. *Macromolecules* **2017**, *50* , 8149-8157.
 106. Fan, B. B.; Ying, L.; Zhu, P.; Pan, F.; Liu, F. L.; Chen, J. W.; Huang, F.; Cao, Y. All-Polymer Solar Cells Based on a Conjugated Polymer Containing Siloxane-Functionalized Side Chains with Efficiency over 10 %. *Adv. Mater.* **2017**, *29* , 1703906.
 107. Li, Z. Y.; Zhong, W. K.; Ying, L.; Liu, F.; Li, N.; Huang, F.; Cao, Y. Morphology optimization via molecular weight tuning of donor polymer enables all-polymer solar cells with simultaneously improved performance and stability. *Nano Energy* **2019**, *64* , 103931.
 108. Fan, B. B.; Du, X. Y.; Liu, F.; Zhong, W. K.; Ying, L.; Xie, R.; Tang, X.; An, K.; Xin, J. M.; Li, N.; Ma, W.; Brabec, C. J.; Huang, F.; Cao, Y. Fine-tuning of the chemical structure of photoactive materials for highly efficient organic photovoltaics. *Nat. Energy***2018**, *3* , 1051-1058.
 109. Fan, B. B.; Zhang, D. F.; Li, M. J.; Zhong, W. K.; Zeng, Z.; Ying, L.; Huang, F.; Cao, Y. Achieving over 16 % efficiency for single-junction organic solar cells. *Sci. China Chem.* **2019**, *62* , 746-752.
 110. Zhu, P.; Fan, B. B.; Du, X. Y.; Tang, X. F.; Li, N.; Liu, F.; Ying, L.; Li, Z.; Zhong, W. K.; Brabec, C. J.; Huang, F.; Cao, Y. Improved Efficiency of Polymer Solar Cells by Modifying the Side Chain of Wide-Band Gap Conjugated Polymers Containing Pyrrolo[3,4-f]benzotriazole-5,7(6H)-dione Moiety. *ACS Appl. Mater. Interfaces* **2018**, *10* , 22495-22503.
 111. Genee, Z.; Negash, A.; Abdulahi, B. A.; Eachambadi, R. T.; Liu, Z.; Van den Brande, N.; D'Haen, J.; Wang, E.; Vandewal, K.; Maes, W.; Manca, J.; Mammo, W.; Admassie, S. Comparative study on the effects of alkylsilyl and alkylthio side chains on the performance of fullerene and non-fullerene polymer solar cells. *Org. Electron.***2020**, *77* .
 112. Li, M. J.; Zeng, Z. Y.; Fan, B. B.; Zhong, W. K.; Zhang, D. F.; Zhang, X.; Zhang, Y.; Ying, L.; Huang, F.; Cao, Y. Tailoring the side chain of imide-functional benzotriazole based polymers to achieve internal quantum efficiency approaching 100 %. *J. Mater. Chem. A***2020**, *8* , 23519-23525.
 113. Fan, B. B.; Li, M. J.; Zhang, D. F.; Zhong, W. K.; Ying, L.; Zeng, Z.; An, K.; Huang, Z.; Shi, L.; Bazan, G. C.; Huang, F.; Cao, Y. Tailoring Regioisomeric Structures of π -Conjugated Polymers Containing Monofluorinated π -Bridges for Highly Efficient Polymer Solar Cells. *ACS Energy Lett.* **2020**, *5* , 2087-2094.
 114. An, K.; Zhong, W. K.; Peng, F.; Deng, W. Y.; Shang, Y.; Quan, H. L.; Qiu, H.; Wang, C.; Liu, F.; Wu, H. B.; Li, N.; Huang, F.; Ying, L. Mastering morphology of non-fullerene acceptors towards long-term stable organic solar cells. *Nat. Commun.* **2023**, *14* , 2688.
 115. Tang, Y.; Xie, L.; Qiu, D.; Yang, C.; Liu, Y.; Shi, Y.; Huang, Z.; Zhang, J.; Hu, J.; Lu, K.; Wei, Z. Optimizing the energy levels and crystallinity of 2,2'-bithiophene-3,3'-dicarboximide-based polymer donors for high-performance non-fullerene organic solar cells. *J. Mater. Chem. C* **2021**, *9* , 7575-7582.
 116. Zhou, N. J.; Guo, X. G.; Ortiz, R. P.; Li, S.; Zhang, S. M.; Chang, R. P. H.; Facchetti, A.; Marks, T. J. Bithiophene Imide and Benzodithiophene Copolymers for Efficient Inverted Polymer Solar Cells. *Adv. Mater.* **2012**, *24* , 2242-2248.
 117. Yang, D. L.; Li, Z. L.; Li, Z. D.; Zhao, X. L.; Zhang, T.; Wu, F.; Tian, Y.; Ye, F.; Sun, Z. Y.; Yang, X. N. Novel wide band gap copolymers featuring excellent comprehensive performance towards the practical application for organic solar cells. *Polym. Chem.***2017**, *8* , 4332-4338.
 118. Zhang, T.; Zeng, G.; Ye, F.; Zhao, X. L.; Yang, X. N. Efficient Non-Fullerene Organic Photovoltaic Modules Incorporating As-Cast and Thickness-Insensitive Photoactive Layers. *Adv. Energy Mater.***2018**, *8* , 1801387.

119. Zhang, T.; Zhao, X.; Yang, D. L.; Tian, Y. M.; Yang, X. N. Ternary Organic Solar Cells with >11 % Efficiency Incorporating Thick Photoactive Layer and Nonfullerene Small Molecule Acceptor. *Adv. Energy Mater.* **2017**, *8* , 1701691.
120. Shi, Y. Q.; Ma, R. J.; Wang, X.; Liu, T.; Li, Y. C.; Fu, S.; Yang, K.; Wang, Y.; Yu, C. J.; Jiao, L.; Wei, X. W.; Fang, J. F.; Xue, D. F.; Yan, H. Influence of Fluorine Substitution on the Photovoltaic Performance of Wide Band Gap Polymer Donors for Polymer Solar Cells. *ACS Appl. Mater. Interfaces* **2022**, *14* , 5740-5749.
121. Yang, J.; Liu, B.; Lee, J. W.; Wang, Y.; Sun, H.; Chen, Z.; Bai, Q.; Kim, B. J.; Jiang, Y.; Niu, L.; Guo, X. Revisiting the Bithiophene Imide-Based Polymer Donors: Molecular Aggregation and Orientation Control Enabling New Polymer Donors for High-Performance All-Polymer Solar Cells. *Chin. J. Chem.* **2022**, *40* , 2900-2908.
122. Guo, X.; Kim, F. S.; Jenekhe, S. A.; Watson, M. D. Phthalimide-Based Polymers for High Performance Organic Thin-Film Transistors. *Journal of the American Chemical Society* **2009**, *131* , 7206-7207
123. Xin, H.; Guo, X.; Kim, F. S.; Ren, G.; Watson, M. D.; Jenekhe, S. A. Efficient solar cells based on a new phthalimide-based donor-acceptor copolymer semiconductor: morphology, charge-transport, and photovoltaic properties. *J. Mater. Chem.* **2009**, *19* , 5303-5310.
124. Du, M. Z.; Chen, Y.; Li, J. F.; Geng, Y. F.; Ji, H. G.; Li, G. Q.; Tang, A.; Guo, Q.; Zhou, E. Wide-Band-Gap Phthalimide-Based D- π -A Polymers for Nonfullerene Organic Solar Cells: The Effect of Conjugated π -Bridge from Thiophene to Thieno[3,2-b]thiophene. *J. Phys. Chem. C* **2019**, *124* , 230-236.
125. Guo, X. J.; Liao, Q. G. D.; Manley, E. F.; Wu, Z.; Wang, Y.; Wang, W.; Yang, T. B.; Shin, Y.-E.; Cheng, X.; Liang, Y. Y.; Chen, L. X.; Baeg, K.-J.; Marks, T. J.; Guo, X. Materials Design via Optimized Intramolecular Noncovalent Interactions for High-Performance Organic Semiconductors. *Chem. Mater.* **2016**, *28* , 2449-2460.
126. Liao, Q. G.; Yang, K.; Chen, J.; Koh, C. W.; Tang, Y. M.; Su, M. Y.; Wang, Y.; Yang, Y. H.; Feng, X. Y.; He, Z.; Woo, H. Y.; Guo, X. G. Backbone Coplanarity Tuning of 1,4-Di(3-alkoxy-2-thienyl)-2,5-difluorophenylene-Based Wide Bandgap Polymers for Efficient Organic Solar Cells Processed from Nonhalogenated Solvent. *ACS Appl. Mater. Interfaces* **2019**, *11* , 31119-31128.
127. Yu, J. W.; Chen, P.; Koh, C. W.; Wang, H.; Yang, K.; Zhou, X.; Liu, B.; Liao, Q. G.; Chen, J. H.; Sun, H. L.; Woo, H. Y.; Zhang, S. M.; Guo, X. G. Phthalimide-Based High Mobility Polymer Semiconductors for Efficient Nonfullerene Solar Cells with Power Conversion Efficiencies over 13 %. *Adv. Sci.* **2018**, *6* , 1801743.
128. Zhang, W. C.; Huang, J. H.; Xu, J. Q.; Han, M. M.; Su, D.; Wu, N. N.; Zhang, C. F.; Xu, A.; Zhan, C. L. Phthalimide Polymer Donor Guests Enable over 17 % Efficient Organic Solar Cells via Parallel-Like Ternary and Quaternary Strategies. *Adv. Energy Mater.* **2020**, *10* , 2001436.
129. Zhang, W. C.; Huang, J. H.; Lv, X. Y.; Zhang, M.; Liu, W.; Xu, T.; Ning, J.; Hexig, A.; Liu, F.; Xu, A.; Zhan, C. Chlorinated phthalimide polymer donor as ultra-wide bandgap and deep HOMO guest for achieving highly efficient polymer solar cells. *Chin. Chem. Lett.* **2023**, *34* , 107436.
130. Li, K.; Wu, Y.; Li, X.; Fu, H.; Zhan, C. 17.1 %-Efficiency organic photovoltaic cell enabled with two higher-LUMO-level acceptor guests as the quaternary strategy. *Sci. China Chem.* **2020**, *63* , 490-496.
131. Arunagiri, L.; Peng, Z.; Zou, X.; Yu, H.; Zhang, G.; Wang, Z.; Lin Lai, J. Y.; Zhang, J.; Zheng, Y.; Cui, C.; Huang, F.; Zou, Y.; Wong, K. S.; Chow, P. C. Y.; Ade, H.; Yan, H. Selective Hole and Electron Transport in Efficient Quaternary Blend Organic Solar Cells. *Joule* **2020**, *4* , 1790-1805.
132. Bi, Z. Z.; Zhu, Q. L.; Xu, X. B.; Naveed, H. B.; Sui, X.; Xin, J. M.; Zhang, L.; Li, T. F.; Zhou, K.; Liu, X. F.; Zhan, X. W.; Ma, W. Efficient Quaternary Organic Solar Cells with Parallel-Alloy Morphology. *Adv. Funct. Mater.* **2019**, *29* , 1806804.
133. Dai, G. L.; Chang, J. J.; Wu, J. S.; Chi, C. Y. Dithieno-naphthalimide based copolymers for air-stable field effect transistors: synthesis, characterization and device performance. *J. Mater. Chem.* **2012**, *22* , 21201.
134. He, B. T.; Tang, L. T.; Zhang, J. M.; Xiao, M. J.; Chen, G. T.; Dai, C. B. A polymer donor based on difluoro-quinoxaline with a naphthalimide substituent unit exhibits a low-lying HOMO level for

- efficient non-fullerene polymer solar cells. *RSC Adv.* **2023**, *13*, 29035-29042.
135. Keshtov, M. L.; Kuklin, S. A.; Konstantinov, I. O.; Khokhlov, A. R.; Nikolaev, A. Y.; Dou, C.; Zou, Y.; Suhtar, R.; Sharma, G. D. New Conjugated Polymers Based on Dithieno[2,3-e:3',2'-g]Isoindole-7,9(8H)-Dione Derivatives for Applications in Nonfullerene Polymer Solar Cells. *Solar RRL* **2019**, *4*, 1900475.
 136. Sun, A. X.; Xu, J. G.; Zong, G. H.; Xiao, Z.; Hua, Y.; Zhang, B.; Ding, L. M. A wide-bandgap copolymer donor with a 5-methyl-4H-dithieno[3,2-e:2',3'-g]isoindole-4,6(5H)-dione unit. *J. Semicond.* **2021**, *42*, 100502.
 137. Li, L. H.; Meng, F.; Zhang, M.; Zhang, Z. G.; Zhao, D. Revisiting the Dithienophthalimide Building Block: Improved Synthetic Method Yielding New High-Performance Polymer Donors for Organic Solar Cells. *Angew. Chem. Int. Ed.* **2022**, *61*, e202206311.
 138. Keshtov, M. L.; Kuklin, S. A.; Zou, Y.; Dahiya, H.; Agrawal, A.; Sharma, G. D. Wide bandgap D-A copolymers with same medium dithieno [2,3-e;3'2'-g]isoindole-7,9 (8H) acceptor and different donors for high-performance fullerene free polymer solar cells with efficiency up to 14.76 %. *Chem. Eng. J.* **2022**, *427*.
 139. Keshtov, M. L.; Konstantinov, I. O.; Kuklin, S. A.; Zou, Y.; Agrawal, A.; Chen, F. C.; Sharma, G. D. Binary and Ternary Polymer Solar Cells Based on a Wide Bandgap D-A Copolymer Donor and Two Nonfullerene Acceptors with Complementary Absorption Spectral. *ChemSusChem* **2021**, *14*, 4731-4740.
 140. Xin, H.; Ge, C.; Jiao, X.; Yang, X.; Rundel, K.; McNeill, C. R.; Gao, X. Incorporation of 2,6-Connected Azulene Units into the Backbone of Conjugated Polymers: Towards High-Performance Organic Optoelectronic Materials. *Angew. Chem. Int. Ed.* **2017**, *57*, 1322-1326.
 141. Zhao, Z.; Zhang, F. J.; Zhang, X.; Yang, X. D.; Li, H. X.; Gao, X. K.; Di, C.-a.; Zhu, D. B. 1,2,5,6-Naphthalenediimide Based Donor-Acceptor Copolymers Designed from Isomer Chemistry for Organic Semiconducting Materials. *Macromolecules* **2013**, *46*, 7705-7714.
 142. Chen, S. C.; Zheng, Q. D.; Zhang, Q. K.; Cai, D. D.; Wang, J. Y.; Yin, Z.; Tang, C. Q. Tuning the frontier molecular orbital energy levels of n-type conjugated copolymers by using angular-shaped naphthalene tetracarboxylic diimides, and their use in all-polymer solar cells with high open-circuit voltages. *Journal of Polymer Science Part A: Polym. Chem.* **2013**, *51*, 1999-2005.
 143. Chen, J. H.; Zhang, X. H.; Wang, G.; Uddin, M. A.; Tang, Y.; Wang, Y.; Liao, Q. G.; Facchetti, A.; Marks, T. J.; Guo, X. G. Dithienylbenzodiimide: a new electron-deficient unit for n-type polymer semiconductors. *J. Mater. Chem. C* **2017**, *5*, 9559-9569.

f

Manuscript received: XXXX, 2023 Manuscript revised: XXXX, 2023 Manuscript accepted: XXXX, 2023 Accepted manuscript

Entry for the Table of Contents

Photo- *Chin. J. Chem.* **2023**, *41*, XXX—XXX. DOI: 10.1002/cjoc.202200XXX

The imide-functionalized polymers are very promising donor materials for non-fullerene OSCs. Aiming to promote future in
